Z. angew. Math. Phys. 53 (2002) 365–406
0044-2275/02/030365-42 $ 1.50+0.20/0

Zeitschrift für angewandte Mathematik und Physik ZAMP

A thermodynamic framework for the study of crystallization in polymers

I. J. Rao and K. R. Rajagopal

Abstract. In this paper, we present a new thermodynamic framework within the context of continuum mechanics, to predict the behavior of crystallizing polymers. The constitutive models that are developed within this thermodynamic setting are able to describe the main features of the crystallization process. The model is capable of capturing the transition from a fluid like behavior to a solid like behavior in a rational manner without appealing to any adhoc transition criterion. The anisotropy of the crystalline phase is built into the model and the specific anisotropy of the crystalline phase depends on the deformation in the melt. These features are incorporated into a recent framework that associates different natural configurations and material symmetries with distinct microstructural features within the body that arise during the process under consideration. Specific models are generated by choosing particular forms for the internal energy, entropy and the rate of dissipation. Equations governing the evolution of the natural configurations and the rate of crystallization are obtained by maximizing the rate of dissipation, subject to appropriate constraints. The initiation criterion, marking the onset of crystallization, arises naturally in this setting in terms of the thermodynamic functions. The model generated within such a framework is used to simulate bi-axial extension of a polymer film that is undergoing crystallization. The predictions of the theory that has been proposed are consistent with the experimental results (see [28] and [7]).

Keywords. Crystallization, natural configurations, material symmetry, semi-crystalline polymers, entropy production.

Introduction

The manner in which a polymer is processed determines its mechanical, optical and electrical properties. Consequently, manufacturing processes have to be designed to fabricate products having the desired properties. Some common examples of processes used to manufacture different polymers are fiber spinning, film blowing, injection molding, blow molding and sheet forming.

The majority of plastic products are manufactured by heating the polymer to above its melting temperature and then cooling it in a mold (e.g., injection molding) or deforming the melt while simultaneously cooling it to get it into the desired shape (e.g., film blowing and fiber spinning). The properties of the final

product depend on the processing conditions the polymer is subjected to during its manufacture, for e.g., in the case of film blowing the crystalline orientation depends on the amount of stretch imparted in the machine direction as well as the transverse direction. Bi-axial extension strengthens the film in the plane, by virtue of which films find widespread use as packaging materials. Uni-axial extension of melts is used to form high strength fibers, in these fibers the polymer molecules crystallize with their backbone parallel to the fiber direction. The successful use of polyester bottles for carbonated drinks was made possible by the development of a special blow molding process that ensures that the polymer in the bottle is bi-axially oriented. At times the crystallization can have detrimental consequences. For instance, the surface layer of an injection-molded article is highly oriented; this can have an adverse effect on the product's quality, for instance it can result in products that are easily cleaved. The above examples illustrate the importance of understanding the phase transition from the melt to a semi-crystalline or amorphous solid as this determines the properties of the final product.

Polymer melts are generally modeled as isotropic viscoelastic liquids. Depending on the molecular structure and processing conditions, the final solid can be either in an amorphous or semi-crystalline state. Polymers that are unable to crystallize, on cooling to below their glass transition temperature form amorphous solids. If these solids are formed by deforming the polymer while cooling through glass transition, they can exhibit anisotropy in their mechanical behavior. As the deformed amorphous polymer melt cools below its glass transition temperature the molecules lose their mobility and are "frozen" in this oriented configuration. Polymers having a regular molecular structure, when kept at temperatures below the melting temperature for a sufficiently long time, form a semi-crystalline solid. Under quiescent conditions the crystallization process can be very slow (especially at temperatures just below the equilibrium melting temperature) and the solid usually has a spherulitic morphology.

The rate of crystallization depends on the molecular orientation in the melt. Subjecting the melt to deformations that align the molecules dramatically increases the rate of crystallization. When the temperature falls below the glass transition temperature there is a cessation of molecular motion and the crystallization process ceases. As the crystallinity increases, it retards the crystallization process, decreasing the mobility of the polymer molecule in the amorphous fraction. A number of polymeric solids like polyethylene find applications at temperatures between their melting temperature and the glass transition temperature. At these temperatures the solid consists essentially of rigid crystals and a flexible amorphous fraction resulting in a solid that is both flexible and tough. The mechanical properties of the final product are dependent on the final morphology of the amorphous and semi-crystalline regions. The morphology in turn depends on the thermal and deformation history undergone by the material during processing. Many products such as fibers and films are subjected to large inelastic deformations after manufacture. During the course of these inelastic deformations, further crystallization

takes place and the morphology and consequently the mechanical behavior evolves with the deformation.

Semi-crystalline polymers have a wide array of uses, ranging from hi-tech applications at one extreme to common everyday applications such as grocery bags at the other extreme. There is no comprehensive theory in place that is capable of predicting the outcome of polymeric processes under different conditions. The problem is vast in its scope and its resolution would require fusing elements of fluid mechanics, solid mechanics, thermodynamics and polymer physics. There is a need for models that can be used in the simulation of the different processes used to manufacture plastics. For instance, for film blowing, polymer companies are able to manufacture different types of resins with differing molecular architectures. However, to determine which of these resins will produce a film having desirable qualities, they need to set up a pilot plant to manufacture large quantities of each resin. Then each resin is blown into film; mechanical tests are subsequently carried out on the film to determine its properties. This process is both expensive and time consuming. Consequently, a model for crystallization which can predict the final properties of the solidified polymer based on the properties of the melt and the processing conditions can increase the efficiency of production and help in designing manufacturing processes that produce components with desirable properties.

The early work on phase transitions was devoted to analyzing problems where conduction was the dominant mechanism. Such studies can be traced back to the works of Lamé [38] and Stefan [67], in which temperature is considered to be the basic variable (see [10], [16], [6], [61]). Another popular approach is the "Phase-Field" model which involves a parameter (other than temperature) called the order parameter. The order parameter takes on extreme values of $+1$ (for pure liquid) and -1 (for pure solid). The heat conduction equation is modified to incorporate the effect of the order parameter that leads to an additional equation whose origin can be traced back to the Landau-Ginzburg theory of phase transitions (see [39]). In most practical situations in which fluid to solid phase transitions take place, several other mechanisms other than conduction come into play, for e.g., convection in the liquid and deformation in the solid. This shortcoming is overcome partially by introducing the kinematics to take into account the flow field (see [21]), however the forming solid is still assumed to be completely quiescent. These approaches result in a model that cannot predict the structural and mechanical properties of the newly formed solid. The ability to predict the properties of the newly formed solid are however essential in all applications, especially so in polymers where the properties of the final solid depend strongly on the processing conditions. Solid – liquid phase transitions present additional challenges as there is a discontinuous transition in the symmetry of the material. Since the issue of symmetry enters the problem only when the kinematical fields of the fluid and solid are taken into account, both the Stefan approach and the Phase-Field approach do not deal with one of the thorniest issues in phase transitions. In many materials

after crystallization is initiated the material goes through an intermediate set of states where it is a mixture of a liquid and solid (a mush) before being completely transformed into a solid. There have been few attempts to describe the mechanics of these mixed regions. A theory of mushy zones has been developed (see [24], [25], [26]) using a mixture theory approach, however, these works do not address the issue of changes in symmetry associated with the phase change and the large deformations of the solid. Baldoni and Rajagopal [5] developed a continuum theory for phase transitions, accounting for changes in symmetry. However, in the specific model developed they assume that the solid is isotropic and the response is like that of a neo- Hookean solid.

In polymers as in other materials, crystallization is first initiated at nucleation sites from which the crystals grow until an equilibrium state is reached. If the nuclei are larger than a critical size, they form stable crystals that grow into the melt. Crystallization ceases when the crystals begin to impinge on one another, reducing the mobility of the polymer chains. The traditional way to model crystallization in polymers is based on the work of Avrami (see [2], [3], [4]). The Avrami equation that has been used widely in modeling quiescent crystallization is based on the theory of filling the space through the nucleation and growth of one phase into another. A discussion of the different variations of the basic Avrami equation to account for isothermal and non-isothermal conditions can be found in a recent detailed review (see [15]). Experimental correlation's for Avrami's equations can be found in the text by Mandelkern [43]. Many polymer-processing applications however take place at very high cooling rates under non-isothermal conditions. Recently, experiments (see [11], [68]) have been carried out to examine the crystallization behavior of polyethylene and polypropylene at high cooling rates. The results show a sharp drop in the temperature till crystallization is initiated, after which there is a plateau region in which vigorous crystallization takes place at a nearly constant temperature, followed by a drop in the temperature to the ambient value after the cessation of crystallization.

In most practical processes, crystallization rarely takes place under quiescent conditions. When the phase transition takes place in a flowing polymer melt, the morphology of the final solid depends on the temperature and deformation history. Crystallization under flow conditions increases the rate of crystallization by orders of magnitude (see [23], [37], [15], [46]). Usually, a highly oriented row-nucleated crystalline morphology is obtained ([32], [31]) in contrast to the spherulitic morphology observed under conditions of quiescent crystallization. The effect of different manufacturing processes on the orientation and morphology has been widely studied (see [50], [73], [74]). In spun fibers the lamellae are found to be perpendicular to the fiber axis and in the case of blown film the lamellae are distributed in the plane of the film. The outer layer of injection molded articles has lamellae oriented perpendicular to both the surface and injection directions while the interior is spherulitic, in the intermediate layers the lamellae remain perpendicular to the surface but lose their preferred orientation with respect to the direction of

injection.

A number of experiments have been conducted concerning crystallization in sheared polymer melts. One of the early experiments concerning crystallization during a simple shear flow between parallel plates was carried out by Haas and Maxwell [23]. In their experiments tiny samples of polyethylene and polybutene-1 (less than 0.5mm thick) were sheared between two parallel glass plates by applying a constant load under isothermal conditions at a temperature below their melting point. At low loads, spherulitic growth was observed while at sufficiently high loads flow induced crystallization was so profuse that no textural detail was observed in the polarizing microscope. Also, the time required for crystallization was orders of magnitude less than that for quiescent crystallization. Similar experiments have been conducted by others (see [30], [49], [37]). Lagasse and Maxwell [37] carried out experiments under conditions of constant shear rate instead of constant load. At low shear rates spherulitic crystallization was observed and at higher shear rates flow induced crystallization was observed, the two regions being clearly demarcated. Enhanced crystallization was determined to be due to chain extension arising from entanglements between molecules. Flow induced crystallization has also been studied in rotational viscometers (see [33], [71], [63], [76]), the results are similar to those obtained in simple shear experiments. In more recent experiments (see [34], [35]) transient shear stresses were imposed on the polymer melt and the microstructural development was monitored in situ using optical and x-ray scattering techniques. The crystallization time was observed to reduce dramatically with the imposition of a brief shear pulse on the melt. Other experiments on flow-induced crystallization have also been carried out in ducts of rectangular cross- section (see [14]). The main conclusion to be gleaned from these works is that the relaxation of the melt has a significant impact on the final thickness of the highly oriented surface layer.

There are not as many extensional flow experiments as shear flow experiments, the main reason being the extreme sensitivity of crystallization to extensional flow, often resulting in flow blockage due to massive crystallization (see [72]). Early work on extensional flows was carried out by Mackley and Keller [41] and Mackley et al. [42], and they reported qualitative rheo-optical characteristics of extensional flow induced crystallization in a confined geometry. In a more recent paper [45] the crystallization of polyethylene was studied in extensional flows by suspending a high-density polyethylene droplet at the stagnation point of a four-roll mill extensional device with linear-low density polyethylene as the carrier phase. The crystallization rate was enhanced by orders of magnitude and the accompanying analysis demonstrates that the melting point elevation model cannot predict the phenomena observed.

From the experiments concerning phase transitions in polymers that crystallize it is clear that the transition from a melt to a semi-crystalline solid is continuous, i.e., during this process the material is a mixture of an amorphous polymer melt and a crystalline solid. On the completion of crystallization the solid that is

formed is a mixture of a crystalline and amorphous solid. Orientation in the melt tremendously accelerates the process of phase transition. However, as the melt is a viscoelastic fluid the orientation of the molecules can either build up or relax depending on the deformation history and the relaxation time of the melt. Orientation of the crystallites formed depends on the orientation of the molecules in the melt just prior to crystallization.

Flow induced crystallization in melts has been modeled in a number of different ways. The classical work of Flory [17] on stress-induced crystallization of rubber has been used to model crystallization of melts. Extension of Flory's work to melts requires the assumption that the temporary network junctions play the same role as the chemical cross-links in the theory of rubber crystallization. Flory's theory rests on the connection between decrease in entropy of the stretched molecule and the tendency of the polymer to crystallize. This work by Flory has been extended by using more complicated expressions for the Helmholtz potential which describe the morphological effects in greater detail (see [20], [19], [64], [65]). Another approach that has been used to model flow induced crystallization is to modify the Avrami equation to account for enhanced crystallization rates due to the flow. In this approach, the effect of flow is built into the equation by the inclusion of an orientation factor, which depends on the flow (see [78], [79], [80], [15], [62]). Recently crystallization in polymers has been modeled using Hamiltonian Poisson bracket formalism (see [9]) and this model has been used to study the fiber-spinning problem [12]. In their model the Avrami equation is used to describe the crystallization kinetics and the equilibrium melting point temperature is used to indicate the onset of crystallization.

Currently there are no theories that can adequately describe the behavior of polymers from the melt like state to the solid state that can take account the evolution of symmetry. Here we will outline the approach that will be used to model the crystallization process described above.

In this paper we propose a methodology for formulating constitutive equations capable of modeling the process of crystallization in polymers. The aim of continuum theories is to describe the macroscopic behavior of a material without explicitly accounting for all the details at the microscopic level. This does not imply that the microstructural processes are ignored, but that the theory deals with these effects in an averaged sense retaining only the salient features. A good understanding of the microstructural mechanisms can aid in formulating better continuum theories. In this work a model is developed using a continuum theory based on the concept of "multiple natural configurations" (multiple stress free states modulo rigid body motions). For materials undergoing large deformations, Eckart [13], seems to have been the first to realize that materials can posses multiple stress free states, that he called "variable relaxed states", and study them in some detail. However, a clear exposition of the central role played by natural configurations in a variety of dissipative processes with associated symmetry changes and the change of the response characteristics of the body have only recently been

demonstrated (see Rajagopal [52]). This approach has been able to explain the material response of a large class of materials under one framework: multi-network theory [51], classical metal plasticity [55], twinning [53], solid to solid phase transitions [56], viscoelastic liquids [57], anisotropic fluids [58] and geological materials [47] have all been modeled within this frame-work and classical elasticity and classical linearly viscous fluids arise naturally as sub-cases. The robustness of this approach in describing the mechanical behavior of a wide array of processes makes it an appropriate choice to model crystallization in polymers. The key feature of this framework is that a body can exist stress free in numerous "natural configurations", the underlying "natural configuration" of the body changing during the process, with the response of the body being elastic from these evolving "natural configurations".

Next, we describe briefly the thermodynamic framework to be used in this work. The internal energy, entropy and rate of dissipation of the material are prescribed and in general depend on the temperature, mass fraction of the crystalline phase and kinematic variables, which are measured from the "natural configurations" of the body. The reduced energy-dissipation equation is used to enforce the second law, this will be explained in greater detail later in the next section. The forms chosen for the constitutive equations are ones that are sufficient to satisfy the second law. We look for sufficient conditions as we are interested in the simplest forms that can model the phenomenon observed. Evolution equations for the natural configuration and mass fraction of the crystalline material are obtained by maximizing the prescribed rate of dissipation and not ad hoc prescriptions.

We discuss the general framework in detail and then derive specific constitutive equations within the framework. The model is used to analyze the bi-axial extension of a film, a deformation that is common in a number of polymer manufacturing processes.

Preliminaries

Consider a body B in a configuration $\kappa_R(B)^*$. Let $\mathbf{X}$ denote a typical position of a material point in κ_R. Let κ_t be the configuration at a time t, then the motion χ_{κ_R} assigns to each particle in configuration a κ_R position in the configuration κ_t at time t, i.e.,

$$\mathbf{x} = \chi_{\kappa_R}(\mathbf{X}, t) \tag{1}$$

The deformation gradient $\mathbf{F}_{\kappa_R}$ is defined through

$$\mathbf{F} := \frac{\partial \chi_{\kappa_R}}{\partial \mathbf{X}}. \tag{2}$$

* We shall, for the ease of notation, use κ_R to mean $\kappa_R(B)$.

The left and right Cauchy-Green stretch tensors $\mathbf{B}_{\kappa_R}$ and $\mathbf{C}_{\kappa_R}$ are defined through

$$\mathbf{B}_{\kappa_R} := \mathbf{F}_{\kappa_R}\mathbf{F}_{\kappa_R}^T, \tag{3}$$

$$\mathbf{C}_{\kappa_R} := \mathbf{F}_{\kappa_R}^T\mathbf{F}_{\kappa_R}. \tag{4}$$

Any acceptable process has to satisfy the appropriate balance laws. The balance equations appropriate for studying the process of crystallization in polymers are the conservation of mass, linear and angular momentum, and energy. We assume that the material is incompressible and that the density of the melt and the semi-crystalline solid are the same. This assumption is made to simplify the problem, in actuality a density change ranging from a few percent to about seven percent has been observed during the transition from melt to solid for different polymers and this can be taken into account by appropriately modifying the theory. The conservation of mass for an incompressible material reduces to

$$\mathrm{div}(\mathbf{v}) = 0, \tag{5}$$

where $\mathbf{v}$ is the velocity. The conservation of linear momentum is

$$\rho\left[\frac{\partial \mathbf{v}}{\partial t} + [\nabla \mathbf{v}]\mathbf{v}\right] = div\mathbf{T} + \rho\mathbf{g}, \tag{6}$$

where $\mathbf{g}$ is the acceleration due to gravity, ρ is the density and $\mathbf{T}$ is the Cauchy stress tensor. For an incompressible material the stress tensor $\mathbf{T}$ reduces to

$$\mathbf{T} = -p\mathbf{I} + \mathbf{T}^E, \tag{7}$$

where p is the Lagrange multiplier due to the constraint of incompressibility, and $\mathbf{T}^E$ is the constitutively determined extra stress. The balance of angular momentum for a body in the absence of internal couples requires that the stress tensor be symmetric. The balance of energy takes the form:

$$\rho\dot{\varepsilon} + \mathrm{div}\,\mathbf{q} = \mathbf{T}\cdot\mathbf{L} + \rho r, \tag{8}$$

where ε is the internal energy,$\mathbf{q}$ is the heat flux vector and r is the radiant heating.

The second law is often introduced in continuum mechanics in the form of the Clausius-Duhem inequality (see [70]). In this work however we will introduce the second law in the form of an equality by introducing a balance law for entropy. This is similar to the approach of Green and Naghdi [22] and Rajagopal and Srinivasa [56]. The balance law for entropy than takes the form

$$\rho\dot{\eta} + \mathrm{div}\left(\frac{\mathbf{q}}{\theta}\right) = \rho\frac{r}{\theta} + \rho\xi, \tag{9}$$

where η is the entropy, θ is the absolute temperature and ξ is the rate of entropy production. Combining the balance of energy, Eq.(8), and the balance of entropy,

Eq. (9) results in the reduced energy-dissipation equation. The reduced energy-dissipation equation is

$$\mathbf{T}\cdot\mathbf{L}-\rho\dot{\varepsilon}+\rho\theta\dot{\eta}-\frac{\mathbf{q}\cdot\operatorname{grad}\theta}{\theta}=+\rho\theta\xi:=\zeta\geq 0, \tag{10}$$

where ζ is the rate of dissipation. Both ξ and ζ are constrained to be non-negative for an acceptable process. Here it should be noted that the rate of dissipation is positive if and only if the rate of entropy production is positive. Sometimes the term, rate of dissipation, is exclusively used to denote the rate of entropy production due to mechanical working. Here we do not use it in such a restrictive sense. As the entropy production can take place because of a variety reasons, for e.g., due to phase change, chemical reactions, heat conduction etc., and not just mechanical working, the rate of dissipation as defined through Eq. (10) is non-zero whenever entropy production is non-zero. On account of this we sometimes use the terms rate of dissipation and rate of entropy production interchangeably with the tacit understanding that the rate of dissipation is defined through the rate of entropy production, as given by Eq. (10). Note that Eq. (10) can be also written as

$$\mathbf{T}\cdot\mathbf{L}-\rho\dot{\psi}-\rho\eta\dot{\theta}-\frac{\mathbf{q}\cdot\operatorname{grad}\theta}{\theta}=\rho\theta\xi:=\zeta\geq 0, \tag{11}$$

where ψ is the Helmholtz potential and is given by $\psi=\varepsilon-\theta\eta$. In this work we use the reduced energy-dissipation equation to place restrictions on the constitutive equations. For reversible processes the rate of entropy production and consequently the rate of dissipation is identically zero. For irreversible processes, to which most thermo- mechanical processes belong the rate of entropy production is greater than zero. In addition it is usually assumed that the rate of dissipation can be split into a part that is due to heat conduction and another part that is a consequence of other irreversible effects, i.e.,

$$\mathbf{T}\cdot\mathbf{L}-\rho\dot{\psi}-\rho\eta\dot{\theta}-\frac{\mathbf{q}\cdot\operatorname{grad}\theta}{\theta}=\rho\theta\xi:=\zeta=\zeta_c+\zeta_d\geq 0, \tag{12}$$

where ζ_c is the rate of dissipation due to heat conduction and ζ_d is the rate of dissipation due to other processes. The rate of dissipation due to heat conduction is assumed to be given by

$$\zeta_c=-\frac{\mathbf{q}\cdot\operatorname{grad}\theta}{\theta}\geq 0. \tag{13}$$

Substituting Eq. (13) into Eq. (12) we obtain

$$\mathbf{T}\cdot\mathbf{L}-\rho\dot{\psi}-\rho\eta\dot{\theta}=\zeta_d\geq 0. \tag{14}$$

As mentioned earlier there can be many different inelastic mechanisms which result in a positive rate of dissipation. In crystallizing polymeric systems the material

starts out as a viscoelastic melt and then crystallizes into a semi-crystalline solid which has an amorphous part and a crystalline part. When the material is a melt the primary source of dissipation is the viscous behavior of the melt. After the onset of crystallization, entropy production takes place not only due to viscous effects in the amorphous phase but is augmented by another term that depends on the crystallization process. Therefore the rate of dissipation due to inelastic processes taking place in the crystallizing polymer are split into

$$\zeta_d = \zeta_a + \zeta_p, \tag{15}$$

where ζ_a is the rate of dissipation due to viscous effects in the amorphous phase and ζ_p is the rate of dissipation due to crystallization. It is also further assumed that each of these mechanisms for entropy production are independent and therefore the associated rates of dissipation are both independently positive, i.e.,

$$\zeta_a \geq 0, \quad \zeta_p \geq 0. \tag{16}$$

Traditionally the second law has been used in the form of the Clausius-Duhem inequality to obtain necessary and sufficient conditions on the forms of the constitutive equations. In those approaches no explicit prescription is usually made for the rate of dissipation. In this work in addition to specifying the internal energy and entropy we also prescribe the rates of dissipation associated with the two different mechanisms. In this we follow the approach used by Rajagopal and Srinivasa [56] who treat the rate of dissipation as a primitive and prescribe a constitutive equation for it. The reduced energy-dissipation equation in the form of Eq. (14) is then used to place restrictions on the constitutive equations. We also use the reduced energy-dissipation equation to obtain sufficient conditions since our primary interest is to deduce the simplest possible forms for the constitutive equations that are capable of describing the physical phenomenon of interest and not the necessarily the most general forms.

The modeling of crystallization can be separated into two main parts, namely, the modeling of the amorphous polymer prior to the onset of crystallization and the modeling of semi-crystalline polymer after crystallization begins.

Modeling of the melt

We model the amorphous state as a viscoelastic fluid using a rate type model. The derivation of the constitutive equations for the stress in a viscoelastic fluid closely follows [57] based on the theory of evolving natural configurations. In this approach the Helmholtz potential and the stress in the fluid are determined from the mapping between the tangent spaces of the natural configuration of the fluid at a material point to the current configuration occupied by it. In figure 1, κ_R is a reference configuration, $\kappa_{c(t)}$ is the configuration currently occupied by the

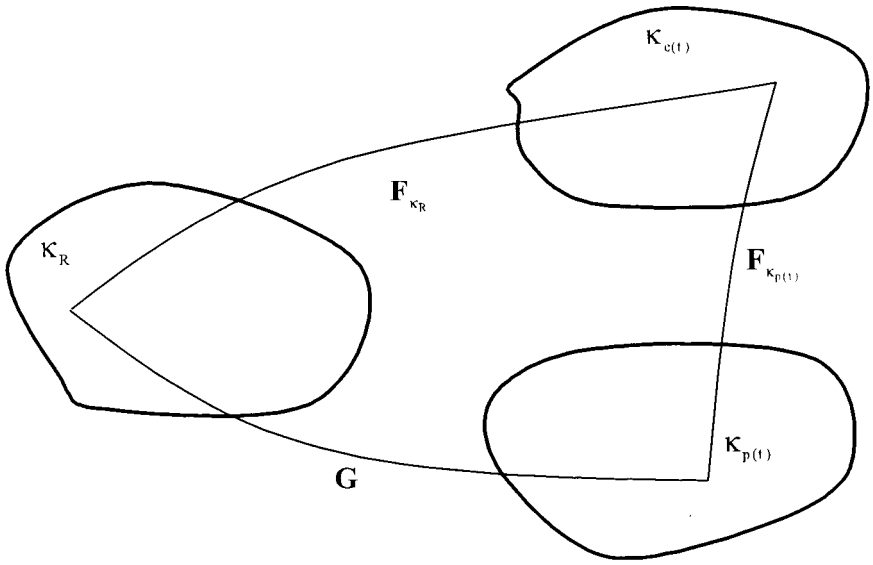

Figure 1. Natural configurations associated with the viscoelastic melt.

material and $\kappa_{p(t)}$ is the natural configuration associated with the material that is currently in the configuration $\kappa_{c(t)}$, that is if the tractions on $\kappa_{c(t)}$ are removed, the body will take the configuration $\kappa_{p(t)}$ (the notation is to suggest the preferred configuration at time t). It is possible for the material to possess more than one natural configuration (see [53], [55], [56], [57], [58], [47], [60], [51], [75], [52]) and in polymeric materials with more than one relaxation mechanism it is common to use models with more than one relaxation time. These models with multiple relaxation times are equivalent to viscoelastic fluid models with multiple sets of natural configurations. Here we shall formulate the model assuming that the melt has multiple relaxation mechanisms.

We assume that the melt has multiple natural configurations associated with it and that it has an instantaneous elastic response from each of these natural configurations. The deformation gradient $\mathbf{F}_{\kappa_R}$ denotes the mapping between the tangent space associated with κ_R, at a point in the reference configuration to the tangent space associated with $\kappa_{c(t)}$. Also, let $\mathbf{F}_{\kappa_{p_i(t)}}$ denote the mapping between the tangent space associated with the configuration $\kappa_{p_i(t)}$, at a material point to the tangent space associated with the current configuration $\kappa_{c(t)}$. Note the index i in $\kappa_{p_i(t)}$ will range from 1 to the number of relaxation mechanisms, n (or the number of natural configurations, denoted here by n) related to the response of the melt. The natural configurations, $\kappa_{p_i(t)}$, are not fixed as in the case of an

elastic solid but evolve as the material is deformed, and this change in the natural configurations is associated with the dissipative response of the material. We also define $\mathbf{G}_i$ to be the mapping between the tangent spaces of κ_R and the natural configuration $\kappa_{p_i(t)}$, i.e.,

$$\mathbf{G}_i := \mathbf{F}_{\kappa_R \to \kappa_{p_i(t)}} = \mathbf{F}^{-1}_{\kappa_{p_i(t)}} \mathbf{F}_{\kappa_R}, \quad i = 1, 2, \ldots, n. \tag{17}$$

We define the velocity gradient, $\mathbf{L}_{\kappa_{p_i(t)}}$, and the symmetric part of $\mathbf{L}_{\kappa_{p_i(t)}}$, $\mathbf{D}_{\kappa_{p_i(t)}}$ to be

$$\mathbf{L}_{\kappa_{p_i(t)}} = \dot{\mathbf{G}}_i \mathbf{G}_i^{-1}, \quad i = 1, 2, \ldots n, \tag{18}$$

$$\mathbf{D}_{\kappa_{p_i(t)}} = \frac{1}{2}\left(\mathbf{L}_{\kappa_{p_i(t)}} + \mathbf{L}^T_{\kappa_{p_i(t)}}\right), i = 1, 2, \ldots n. \tag{19}$$

In this approach the left Cauchy Stretch tensors $\mathbf{B}_{\kappa_{p_i(t)}}$ play the role of physically motivated internal variables. When crystallization is initiated the orientation of the crystals and consequently their mechanical response is anisotropic. The induced anisotropy depends on the direction in which the molecules in the melt have been extended. The tensors $\mathbf{B}_{\kappa_{p_i(t)}}$ contain information about the orientation of the molecules in the melt, albeit in an averaged way. We shall use these tensors to determine the direction of anisotropy in the crystalline solid that is formed. The manner in which this is implemented is discussed in detail in the next section.

Using the definition of $\mathbf{B}_{\kappa_{p_i(t)}}$, Eq. (17) and Eq. (19) it is easy to show that

$$\overset{\triangledown}{\mathbf{B}}_{\kappa_{p_i(t)}} := \dot{\mathbf{B}}_{\kappa_{p_i(t)}} - \mathbf{L}\mathbf{B}_{\kappa_{p_i(t)}} - \mathbf{B}_{\kappa_{p_i(t)}}\mathbf{L}^T = -2\mathbf{F}_{\kappa_{p_i(t)}}\mathbf{D}_{\kappa_{p_i(t)}}\mathbf{F}^T_{\kappa_{p_i(t)}}, \quad i = 1, 2, \ldots n. \tag{20}$$

where the inverted triangle denotes the upper convected Oldroyd derivative and the dot is the material time derivative. Specification of $\mathbf{D}_{\kappa_{p_i(t)}}$ is tantamount to prescribing the manner in which the underlying natural configurations evolve. As the material is incompressible we shall assume that the motion associated with these natural configurations are isochoric, i.e.,

$$\mathrm{tr}\left(\mathbf{D}_{\kappa_{p_i(t)}}\right) = 0, \quad i = 1, 2, \ldots n. \tag{21}$$

We derive the forms for $\mathbf{D}_{\kappa_{p_i(t)}}$, using the second law in the form of the reduced energy- dissipation equation and by requiring that the rate of dissipation be maximized.

We assume that the internal energy and the entropy of the melt depend on the temperature and the mappings $\mathbf{F}_{\kappa_{p_i(t)}}$, $i = 1, 2, \ldots n$, i.e.,

$$\varepsilon_a = \varepsilon_a(\theta, \mathbf{F}_{\kappa_{p_1(t)}}, \mathbf{F}_{\kappa_{p_2(t)}}, \ldots, \mathbf{F}_{\kappa_{p_n(t)}}), \tag{22}$$

$$\eta_a = \eta_a(\theta, \mathbf{F}_{\kappa_{p_1(t)}}, \mathbf{F}_{\kappa_{p_2(t)}}, \ldots, \mathbf{F}_{\kappa_{p_n(t)}}). \tag{23}$$

The above forms can be further simplified since the melt is isotropic and incompressible, due to which the internal energy and entropy depend on $\mathbf{F}_{\kappa_{p_i(t)}}$ through the first two invariants of $\mathbf{B}_{\kappa_{p_i(t)}}$, i.e.,

$$I_i = \operatorname{tr}\left(\mathbf{B}_{\kappa_{p_i(t)}}\right), \quad II_i = \operatorname{tr}\left(\mathbf{B}^2_{\kappa_{p_i(t)}}\right), \quad i = 1, 2, \dots n. \tag{24}$$

Therefore the internal energy and entropy have the forms

$$\varepsilon_a = \varepsilon_a(\theta, I_1, II_1, I_2, II_2, \dots, I_n, II_n), \tag{25}$$
$$\eta_a = \eta_a(\theta, I_1, II_1, I_2, II_2, \dots, I_n, II_n), \tag{26}$$

and consequently the Helmholtz potential has the following form

$$\psi_a = \psi_a(\theta, I_1, II_1, I_2, II_2, \dots, I_n, II_n). \tag{27}$$

Also because the melt is isotropic the configurations $\kappa_{p_i(t)}$ can be chosen such that

$$\mathbf{F}_{\kappa_{p_i(t)}} = \mathbf{V}_{\kappa_{p_i(t)}}, \quad i = 1, 2, \dots n. \tag{28}$$

We also assume that the dissipation in the melt is due to the effect of viscosity and that the rate of dissipation has the form:

$$\zeta_d = \zeta_a(\theta, \mathbf{B}_{\kappa_{p_1(t)}}, \dots, \mathbf{B}_{\kappa_{p_n(t)}}, \mathbf{D}_{\kappa_{p_1(t)}}, \dots, \mathbf{D}_{\kappa_{p_i(t)}}), \tag{29}$$

where ζ_a is the rate of dissipation. When the underlying natural configurations do not change, i.e., when $\mathbf{D}_{\kappa_{p_i(t)}}$ are null tensors ($\mathbf{D}_{\kappa_{p_i(t)}} = \mathbf{0}$, $i = 1, 2, \dots n.$) the rate of dissipation ζ_a is expected to be identically zero. This is the case during rapid processes wherein the melt behaves like an elastic solid. Substituting these forms into the reduced energy dissipation equation, Eq. (14), and using Eq. (20) and Eq. (27) and Eq. (29) we get

$$\begin{aligned}\left(\mathbf{T} - \sum_{i=1}^{n} 2\rho\left[\frac{\partial\psi_a}{\partial I_i}\mathbf{B}_{\kappa_{p_i(t)}} + 2\frac{\partial\psi_a}{\partial II_i}\mathbf{B}^2_{\kappa_{p_i(t)}}\right]\right)\cdot\mathbf{D} + \\ \sum_{i=1}^{n} 2\rho\left[\frac{\partial\psi_a}{\partial I_i}\mathbf{B}_{\kappa_{p_i(t)}} + 2\frac{\partial\psi_a}{\partial II_i}\mathbf{B}^2_{\kappa_{p_i(t)}}\right]\cdot\mathbf{D}_{\kappa_{p_i(t)}} \\ - \left(\frac{\partial\psi_a}{\partial\theta} + \eta_a\right)\dot{\theta} = \zeta_a \geq 0.\end{aligned} \tag{30}$$

Since we are looking for forms that are sufficient to satisfy the above equation it seems reasonable to assume that the stress is given by

$$\mathbf{T} = -p\mathbf{I} + \sum_{i=1}^{n} 2\rho\left[\frac{\partial\psi_a}{\partial I_i}\mathbf{B}_{\kappa_{p_i(t)}} + 2\frac{\partial\psi}{\partial II_i}\mathbf{B}^2_{\kappa_{p_i(t)}}\right], \tag{31}$$

and that the Helmholtz potential and the entropy are related through

$$\frac{\partial \psi_a}{\partial \theta} = -\eta_a, \tag{32}$$

where p is the Lagrange multiplier due to the constraint of incompressibility. Equation (31) is sufficient to ensure that for all motions for which there is no change in the natural configuration the material behaves elastically. Also Eq. (32) is equivalent to the following relationship between the internal energy and the entropy

$$\frac{\partial \varepsilon_a}{\partial \theta} = \theta \frac{\partial \eta_a}{\partial \theta}. \tag{33}$$

Substituting Eq. (31) and Eq. (32) into Eq. (30) we get

$$\sum_{i=1}^{n} \mathbf{T}_i \cdot \mathbf{D}_{\kappa_{p_i(t)}} = \zeta_a \geq 0, \tag{34}$$

where the partial stress is given by

$$\mathbf{T}_i = 2\rho \left[\frac{\partial \psi_a}{\partial I_i} \mathbf{B}_{\kappa_{p_i(t)}} + 2 \frac{\partial \psi}{\partial II_i} \mathbf{B}^2_{\kappa_{p_i(t)}} \right], \quad i = 1, 2, \ldots n. \tag{35}$$

Equation (34) places restrictions on the tensors $\mathbf{D}_{\kappa_{p_i(t)}}$, $i = 1, 2, \ldots n$. We assume (similar to [57]) that the actual values of $\mathbf{D}_{\kappa_{p_i(t)}}$, $i = 1, 2, \ldots n$ chosen satisfy the constraints given by Eq. (34) and Eq. (21) and also corresponds to a maximum for the rate of dissipation. This is enforced using the method of Lagrange multipliers by extremizing the rate of dissipation, given by Eq. (29), subject to the constraints Eq.(34) and Eq. (21). On doing this we obtain the following equations for determining $\mathbf{D}_{\kappa_{p_i(t)}}$,

$$\mathbf{T}_i = \beta_{1i} \frac{\partial \zeta_a}{\partial \mathbf{D}_{\kappa_{p_i(t)}}} - \beta_{2i} \mathbf{I} = \mathbf{0}, i = 1, 2, \ldots n. \tag{36}$$

where β_{1i} and β_{2i}, $i = 1, 2, \ldots n$ are Lagrange multipliers which are associated with the constraints that are enforced. Using Eq. (36) and Eq. (31) we can obtain equations for $\mathbf{D}_{\kappa_{p_i(t)}}$, which contain information about the evolution of the different natural configurations associated with the melt. To proceed further with the derivation and to formulate specific constitutive equations we need to prescribe specific forms for the thermodynamic functions, i.e., the internal energy, ε, the entropy, η, and the rate of dissipation, ζ_a.

In polymer melts as in the case of rubber, deformation strongly affects the configurational entropy while the internal energy does not change significantly. In light of this it is reasonable to assume that the internal energy is a function of

only the temperature while the entropy depends on both the temperature and the invariants of $\mathbf{B}_{\kappa_{p_i(t)}}$, i.e.,

$$\varepsilon_a = \varepsilon_a(\theta)^\dagger, \tag{37}$$

$$\eta_a = \eta_a(\theta, I_1, II_1, \ldots, I_n, II_n). \tag{38}$$

We further assume that the entropy of the melt satisfies an additive split into a part that depends only on temperature and another part that depends only on the deformation.

$$\eta_a = \hat{\eta}_a(\theta) + \sum_{i=1}^{n} \tilde{\eta}_a(I_i, II_i). \tag{39}$$

For the part of the entropy that depends on the deformation, we chose a form consistent with that of a mixture of neo-Hookean materials, i.e.,:

$$\eta_a = \hat{\eta}_a(\theta) - \sum_{i=1}^{n} \bar{\mu}_i(I_i - 3). \tag{40}$$

If the internal energy can be represented, in the temperature range of interest, as a linear function of the temperature, then

$$\varepsilon_a = C_a\theta + A_a, \tag{41}$$

where C_a is the specific heat of the amorphous melt and A_a is a constant. The corresponding form for the entropy reduces to:

$$\eta_a = C_a \ln(\theta) + B_a - \sum_{i=1}^{n} \bar{\mu}_i(I_i - 3), \tag{42}$$

where B_a is a constant and $\bar{\mu}_i$, $i = 1, 2, \ldots n$, are material constants related to the shear moduli associated with the different relaxation mechanisms. The forms chosen in Eq. (41) and Eq. (42) satisfy the constraint given by Eq. (32). Substituting the forms chosen for the entropy and internal energy into Eq. (31), we get the following equation for the stress,

$$\mathbf{T} = -p\mathbf{I} + \sum_{i=1}^{n} \mu_i \mathbf{B}_{\kappa_{p_i(t)}}, \tag{43}$$

with the shear moduli of the melt, μ_i, given by

$$\mu_i = 2\rho\theta\bar{\mu}_i, \quad i = 1, 2, \ldots n. \tag{44}$$

[†]In general the internal energy can also depend on the deformation through the invariants of $\mathbf{B}_{\kappa_{p_i(t)}}$.

The form for the stress given by Eq. (43) is identical to that of a mixture of neo-Hookean materials. This represents the elastic response of the body. However, its dissipative response determines the evolution of the natural configurations. As in rubber elasticity, we shall assume that the shear moduli are linearly dependent on the temperature. The rate of dissipation is assumed to have the following form.

$$\zeta_a = \sum_{i=1}^{n} 2\nu_i \mathbf{D}_{\kappa_{p_i(t)}} \cdot \mathbf{B}_{\kappa_{p_i(t)}} \mathbf{D}_{\kappa_{p_i(t)}}, \tag{45}$$

where ν_i[‡] is the viscosity associated with the ith relaxation mechanism and can depend in general on both the temperature and the deformation through the tensor $\mathbf{B}_{\kappa_{p_i(t)}}$, i.e.,

$$\nu_i = \nu_i(\theta, \mathbf{B}_{\kappa_{p_i(t)}}), \quad i = 1, 2, \ldots n. \tag{46}$$

Substituting Eq. (45) into Eq. (36) and eliminating β_{1i} by using Eq. (21) and Eq. (34) we obtain

$$\mathbf{T}_i = 2\nu_i \mathbf{B}_{\kappa_{p_i(t)}} \mathbf{D}_{\kappa_{p_i(t)}} + \beta_{2i}\mathbf{I}, i = 1, 2, \ldots n. \tag{47}$$

From Eq. (43) and Eq. (47) and using Eq. (21), we obtain the following equation for $\mathbf{D}_{\kappa_{p_i(t)}}$,

$$\mathbf{D}_{\kappa_{p_i(t)}} = \frac{\mu_i}{2\nu_i} \left(\mathbf{I} - \frac{3}{\mathrm{tr}(\mathbf{B}^{-1}_{\kappa_{p_i(t)}})} \mathbf{B}^{-1}_{\kappa_{p_i}(t)} \right), i = 1, 2, \ldots n. \tag{48}$$

Substituting Eq. (48) into Eq. (20) we obtain the evolution equation for $\mathbf{B}_{\kappa_{p_i(t)}}$ as

$$\overset{\nabla}{\mathbf{B}}_{\kappa_{p_i(t)}} := \dot{\mathbf{B}}_{\kappa_{p_i(t)}} - \mathbf{L}\mathbf{B}_{\kappa_{p_i(t)}} - \mathbf{B}_{\kappa_{p_i(t)}}\mathbf{L}^T = \frac{\mu_i}{\nu_i} \left(\frac{3}{\mathrm{tr}(\mathbf{B}^{-1}_{\kappa_{p_i(t)}})} \mathbf{I} - \mathbf{B}_{\kappa_{p_i(t)}} \right), \quad i = 1, 2, \ldots n. \tag{49}$$

The ratio of the viscosity, ν_i, to the shear modulus , μ_i, has units of time and is known as the relaxation time, λ_i, i.e.,

$$\lambda_i = \frac{\nu_i}{\mu_i}, \ i = 1, 2, \ldots n. \tag{50}$$

[‡] Usually in fluid dynamics ν is used to denote the kinematic viscosity and η or μ normally denotes the dynamic viscosity. In this work, however, we use ν to denote the dynamic viscosity in order to avoid any confusion with the entropy, η, or the shear modulus, μ.

Finally we obtain the energy equation by substituting the internal energy given by Eq. (37) into the energy equation, Eq. (8) to give

$$\rho\frac{\partial\varepsilon}{\partial\theta}\dot{\theta} + \operatorname{div}\mathbf{q} = \mathbf{T}\cdot\mathbf{L} + \rho r. \tag{51}$$

This can be further simplified by using the specific form for the internal energy given by Eq. (41), this results in

$$\rho C_a\dot{\theta} + \operatorname{div}\mathbf{q} = \mathbf{T}\cdot\mathbf{L} + \rho r. \tag{52}$$

This completes the development of the constitutive theory for the melt.

At this juncture it would be appropriate to point out that models similar to the one derived in this section have been investigated by Leonov and Prokunin [40] using non-equilibrium thermodynamics. However, the methodology used to develop the constitutive equations in our work is very different and is the part of a much more general framework, which as we shall see in the next section can account for symmetry changes that are observed in crystallization. Also the thermo-mechanical framework is quite different and more importantly, the significance attached to many of the quantities are quite different. In yet another approach, viscoelastic fluids are modeled using an internal variable called the configuration tensor. In viscoelastic fluid models based on the configuration tensor, the stress is related to the configuration tensor in the same way as in Eq. (43), i.e., with $\mathbf{B}_{\kappa_{p_i(t)}}$ (for a model with a single relaxation time) replaced by configuration tensor. In these models an evolution equation is prescribed for the configuration tensor. More details concerning these models can be found in [40]. The main difference between these two approaches is the meaning given to $\mathbf{B}_{\kappa_{p_i(t)}}$ and the configuration tensor. The tensor $\mathbf{B}_{\kappa_{p_i(t)}}$ has a specific kinematic meaning, which implies that it satisfies the constraint due to incompressibility, i.e.,

$$\det(\mathbf{B}_{\kappa_{p_i(t)}}) = 1. \tag{53}$$

The configuration tensor however does not satisfy any such a constraint. Just as in the case of the tensor $\mathbf{B}_{\kappa_{p_i(t)}}$, the configuration tensor contains information about the orientation and stretch of the polymer molecules, albeit in an averaged sense, but it will lack appropriate physical meaning or a proper thermodynamic framework. In the next section we shall augment the model developed in this section to incorporate the presence of the crystalline phase.

Modelling of the amorphous-crystalline mixture

Crystallization can be initiated in polymers either due to changes in temperature (by cooling) or by deformation. In this section we first develop the structure of the

thermodynamic quantities such as entropy, internal energy and rate of dissipation, from which follow the forms for the stress tensor, crystallization rate and a criterion for the initiation of crystallization. These constitutive equations are applicable to general crystallizing polymers. The framework is general enough that specific details of different polymers can be added to the model.

After the onset of crystallization the material is a mixture of an amorphous phase and a crystalline phase. The presence of the crystalline phase effects the response of the material. We treat the mixture of the crystalline and amorphous phases as a constrained mixture. We allow for the co-occupancy of the phases in an averaged sense reminiscent of traditional mixture theory (see [69], [8], [1], [54]). We assume that the amorphous and crystalline components are constrained to move together, i.e., the two phases do not diffuse relative to each other. For polymers this is a reasonable assumption as the same molecule traverses both the amorphous and crystalline phase and the crystalline phase pins down the molecule preventing it from diffusing.

The newly formed crystalline material is assumed to be an elastic solid. For elastic solids the stress depends on the deformation gradient from a configuration of known stress (usually a stress free configuration) and the current configuration. Here we assume that the crystalline material is born in a stress free state. This is similar to the approach used by Rajagopal and Wineman [51] for their multi-network theory for polymers. As further deformation takes place this newly formed solid is deformed. The solid that is subsequently formed is also born in a stress free state. The crystallized solid can be thought of as a mixture of elastic solids with different natural configurations. The stress free configuration of the solid fraction born at some time t is the configuration of the body at the time t. If solidification is initiated at time τ_s, in figure 2, let τ be some time later than τ_s at which solidification is taking place. We assume that the thermodynamic quantities, the internal energy and entropy (at time t) in the body due to the solid fraction born at time τ is determined by the deformation gradient from the configuration of the body at time τ to the current configuration at time t, i.e., $\mathbf{F}_{\kappa_{c(\tau)}}$, while the internal energy and entropy of the amorphous phase are determined by $\mathbf{F}_{\kappa_{p_i(t)}}$, $i = 1, \dots n.$ through $\mathbf{B}_{\kappa_{p_i(t)}}$, $i = 1, \dots n$. Note, in figure 2 we illustrate this with an amorphous phase having a single relaxation mechanism. With these assumptions the internal energy and entropy of the newly formed crystalline phase are given by

$$\varepsilon_c = \varepsilon_c(\theta, \mathbf{F}_{\kappa_{c(\tau)}}), \tag{54}$$

$$\eta_c = \eta_c(\theta, \mathbf{F}_{\kappa_{c(\tau)}}). \tag{55}$$

The above assumptions imply that the crystalline phase is an elastic solid. The assumption of Material Frame Indifference places additional restrictions on the form of ε_c and η_c in that they depend on $\mathbf{F}_{\kappa_{c(\tau)}}$ through the right Cauchy stretch tensor, $\mathbf{C}_{\kappa_{c(\tau)}}$, i.e.,

$$\varepsilon_c = \varepsilon_c(\theta, \mathbf{C}_{\kappa_{c(\tau)}}), \tag{56}$$

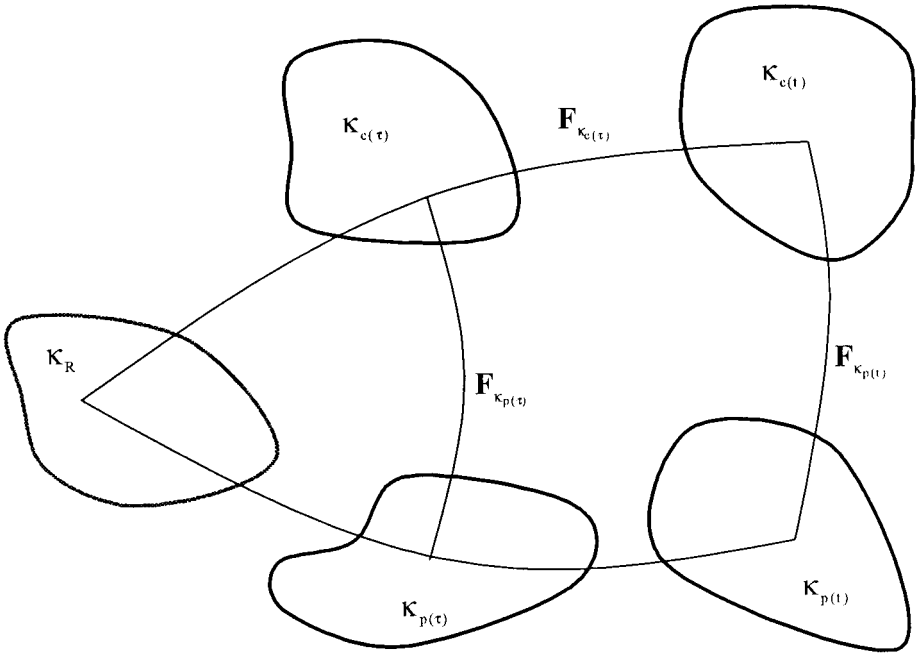

Figure 2. Natural configurations associated with the crystallizing fluid–solid mixture.

$$\eta_c = \eta_c(\theta, \mathbf{C}_{\kappa_{c(\tau)}}). \tag{57}$$

The Helmholtz potential will also have the same dependence on $\mathbf{C}_{\kappa_{c(\tau)}}$,

$$\psi_c = \psi_c(\theta, \mathbf{C}_{\kappa_{c(\tau)}}). \tag{58}$$

In polymers, as we have discussed earlier, the anisotropy in the solid that is formed depends on the orientation of the molecules in the melt at the time of crystallization. The tensors $\mathbf{B}_{\kappa_{p_i(\tau)}}$, $i = 1, \ldots n$, give us information about the orientation of the molecules in the melt at time $t = \tau$, albeit in an averaged sense. If a melt can be described by a single relaxation mechanism, i.e., it has one relaxation time associated with it, then the three principal directions of $\mathbf{B}_{\kappa_{p(\tau)}}$ give us the directions of the principal stretchs in the melt. Experiments suggest that we can use these mutually perpendicular principal directions to determine the directions of anisotropy in the solid. The principal directions can be quantified by any two of the three eigenvectors of $\mathbf{B}_{\kappa_{p(\tau)}}$, namely $\mathbf{n}_{\kappa_{c(\tau)}}$ and $\mathbf{m}_{\kappa_{c(\tau)}}$ (see [59]). In the more general case wherein the melt is described by a number of natural configurations, i.e., a number of relaxation mechanisms, the situation is not as transparent. In this case the orientation of the molecules is represented by

the tensors $\mathbf{B}_{\kappa_{p_i(\tau)}}$, $i = 1, \ldots n$. This information can be used to determine the orientation of crystalline phase in a number of ways, for e.g., the orientation of the crystalline phase can be determined by the eigenvectors associated with one of the n tensors, $\mathbf{B}_{\kappa_{p_i(\tau)}}$, $i = 1, \ldots n$. This was done by Rao and Rajagopal [60] while modeling crystallization in polyethylene terephthalate (PET) films, wherein the behavior of PET was described using a model with two relaxation times. In that work the orientation of the crystalline phase was determined from the eigenvectors of the tensor $\mathbf{B}_{\kappa_{pn(t)}}$ associated with the largest relaxation time, here we shall do the same. The symmetry group of an orthotropic solid is determined by three mutually perpendicular directions, and it is this form of anisotropy that seems appropriate for the solid formed under conditions of unequal stretch in three principal directions. For this reason, we assume that the elastic solid that is formed at each instant is an orthotropic elastic solid. The three principal directions of the orthotropic solid formed at time $t = \tau$ are determined by $\mathbf{n}_{\kappa_{c(\tau)}}$ and $\mathbf{m}_{\kappa_{c(\tau)}}$ and in general can change with time. Thus we assume that the functional form for the Helmholtz potential is consistent with that of an orthotropic solid with respect to the configuration $\kappa_{c(\tau)}$. The directions associated with $\mathbf{n}_{\kappa_{c(\tau)}}$ and $\mathbf{m}_{\kappa_{c(\tau)}}$ are used in order to incorporate the dependence of anisotropy in the elastic response of the crystalline solid. The Helmholtz potential of an incompressible orthotropic elastic solid depends on the first two invariants of the right Cauchy-Green stretch tensor, ,which we denote by I_C, II_C, and the following scalars (see [66]):

$$J_1 = \mathbf{n}_{\kappa_{c(\tau)}} \cdot \mathbf{C}_{\kappa_{c(\tau)}} \mathbf{n}_{\kappa_{c(\tau)}}, \quad K_1 = \mathbf{m}_{\kappa_{c(\tau)}} \cdot \mathbf{C}_{\kappa_{c(\tau)}} \mathbf{m}_{\kappa_{c(\tau)}},$$

$$J_2 = \mathbf{n}_{\kappa_{c(\tau)}} \cdot \mathbf{C}^2_{\kappa_{c(\tau)}} \mathbf{n}_{\kappa_{c(\tau)}}, \quad K_2 = \mathbf{m}_{\kappa_{c(\tau)}} \cdot \mathbf{C}^2_{\kappa_{c(\tau)}} \mathbf{m}_{\kappa_{c(\tau)}}, \tag{59}$$

The most general form of the Helmholtz potential for an orthotropic elastic solid can then be written as:

$$\psi_c = \psi_c(\theta, I_C, II_C, J_1, J_2, K_1, K_2), \tag{60}$$

where the invariants depend on t and τ. It is worth noting here that this is not the only way in which anisotropy in the solid that is formed can depend on the fluid motion. Alternate ways of inducing the anisotropy can be easily included, however, their forms will have to be motivated by experimental data. It should be recognized that ε_c and η_c can also depend on the conditions in the melt at the instant of formation through the eigenvalues or the invariants of the tensors $\mathbf{B}_{\kappa_{p_i(\tau)}}$, $i = 1, \ldots n$.

The entropy and internal energy for the mixture are assumed to be additive, i.e., they take the form:

$$\varepsilon = \int_{\tau_s}^{t} \varepsilon_c \frac{d\alpha}{d\tau} d\tau + i_\varepsilon + (1 - \alpha)\varepsilon_a, \tag{61}$$

$$\eta = \int_{\tau_s}^{t} \eta_c \frac{d\alpha}{d\tau} d\tau + i_\eta + (1-\alpha)\eta_a, \tag{62}$$

where i_ε is the interfacial energy per unit mass of the amorphous-crystalline mixture and i_η is the interfacial entropy per unit mass of the amorphous-crystalline mixture. These interfacial components are added to take into account the presence of phase boundaries. These phase boundaries will lead to a deviation of the properties of the mixture from that of the averaged properties of the pure amorphous and crystalline phase. This is because their presence will change the structure of the amorphous and crystalline regions in the vicinity of the interface. In polymers this term is expected to be important as the crystalline lamellae are small and there is a substantial amount of material in the interfacial region in between the crystalline and amorphous regions (see [44], [18], [36]). Also, ε_a and η_a are assumed to have the same form as that for the melt and are given by Eq. (25) and Eq. (26) respectively. The Helmholtz potential for the mixture is then given by

$$\psi = \int_{\tau_s}^{t} \psi_c \frac{d\alpha}{d\tau} d\tau + i_\psi + (1-\alpha)\psi_a. \tag{63}$$

Note, that in the above equation for the Helmholtz potential for the mixture in Eq. (61) and Eq. (62) for the internal energy and entropy of the mixture there is an integral as the crystalline phase is formed gradually and not at an instant. In addition the forms for ε_c, η_c and ψ_c can in general be different for the crystalline material formed at different times.

Now we specify the rate of dissipation. There is dissipation in the material due to the viscosity of the amorphous phase, on the other hand, the crystalline phase formed is assumed to be elastic and hence there is no dissipation associated with the deformation of the crystalline phase. The process of crystallization is an entropy producing process. This can be discerned clearly from the experiments carried out on the quiescent crystallization of polyethylene where the material is first cooled till it crystallizes and is subsequently heated to a melt like state. The temperatures at which the majority of the crystallization takes place is lower than the temperature at which melting takes place, a clear indicator of a entropy producing process as the state of the melt before and after the crystallization-melting cycle is the same. We assume that the rate of dissipation can be split into two parts, the first related to the dissipation due to the viscous effects in the amorphous phase and the second related to the phase change, i.e.,

$$\zeta_d = \zeta_a + \zeta_p, \tag{64}$$

where ζ_a is the rate of dissipation due to viscous effects in the amorphous phase and ζ_p is the rate of dissipation due to crystallization. We assume that both ζ_a and ζ_p are individually non negative. We expect the rate of dissipation of the

amorphous phase, ζ_a to have a form similar to that for a purely amorphous phase and therefore assume that it is given by

$$\zeta_a = \zeta_a(\alpha, \theta, \mathbf{B}_{\kappa_{p_1(t)}}, \ldots, \mathbf{B}_{\kappa_{p_n(t)}}, \mathbf{D}_{\kappa_{p_1(t)}}, \ldots, \mathbf{D}_{\kappa_{p_n(t)}}). \tag{65}$$

Note that ζ_a in the above equation also depends on the crystallinity, α. As in the case of the melt we stipulate that when the underlying natural configurations do not change, i.e., when $\mathbf{D}_{\kappa_{p_i(t)}}$ are null tensors ($\mathbf{D}_{\kappa_{p_i(t)}} = \mathbf{0}$, $i = 1, ..n$), then the rate of dissipation due to viscous effects in the amorphous phase, ζ_a is identically zero.

Next, we assume that ζ_p depends on the crystallinity, α, the rate of change of crystallinity, $\dot{\alpha}$ and the temperature, θ and in addition it can depend on other kinematic variables i.e.,

$$\zeta_p = \zeta_p(\theta, \alpha, \dot{\alpha} \ldots) \geq 0. \tag{66}$$

The rate of dissipation due to crystallization, ζ_p, has to be exactly zero when no crystallization is taking place, i.e.,

$$\zeta_p\big|_{\dot{\alpha}=0} = 0. \tag{67}$$

Substituting the Helmholtz potential from Eq. (63) with ψ_a given by Eq. (27) and ψ_c given by Eq. (60) and the forms for the rate of dissipation with ζ_a given by Eq. (65) and ζ_p given by Eq. (66) into the reduced energy dissipation equation , Eq. (14) we obtain

$$\begin{aligned}
&\left(\mathbf{T} - \sum_{i=1}^{n}(1-\alpha)2\rho\left[\frac{\partial\psi_a}{\partial I_i}\mathbf{B}_{\kappa_{p_i(t)}} + 2\frac{\partial\psi_a}{\partial II_i}\mathbf{B}^2_{\kappa_{p_i(t)}}\right]\right.\\
&\qquad\left. -2\rho\left[\int_{\tau_s}^{t}\mathbf{F}_{\kappa_{c(\tau)}}\frac{\partial\psi_c}{\partial\mathbf{C}_{\kappa_{c(\tau)}}}\mathbf{F}^T_{\kappa_{c(\tau)}}\frac{d\alpha}{d\tau}d\tau\right]\right)\cdot\mathbf{D} +\\
&\sum_{i=1}^{n}(1-\alpha)\left(2\rho\left[\frac{\partial\psi_a}{\partial I_i}\mathbf{B}_{\kappa_{p_i(t)}} + 2\frac{\partial\psi_a}{\partial II_i}\mathbf{B}^2_{\kappa_{p_i(t)}}\right]\cdot\mathbf{D}_{\kappa_{p_i(t)}}\right) - \left(\frac{\partial\psi}{\partial\theta} + \eta\right)\dot{\theta} +\\
&\qquad\rho\left(\psi_a - \psi_c\big|_{\mathbf{C}_{\kappa_{c(t)}}=\mathbf{I}} - \frac{\partial i_\psi}{\partial\alpha}\right)\dot{\alpha} = \zeta_a + \zeta_p \geq 0.
\end{aligned} \tag{68}$$

We shall look for a form for the stress that is sufficient to satisfy the above equation, we shall assume that the stress is given by

$$\begin{aligned}
\mathbf{T} = -p\mathbf{I} &+ \sum_{i=1}^{n}2(1-\alpha)\rho\left[\frac{\partial\psi_a}{\partial I_i}\mathbf{B}_{\kappa_{p_i(t)}} + 2\frac{\partial\psi_a}{\partial II_i}\mathbf{B}^2_{\kappa_{p_i(t)}}\right] +\\
&2\rho\left[\int_{\tau_s}^{t}\mathbf{F}_{\kappa_{c(\tau)}}\frac{\partial\psi_c}{\partial\mathbf{C}_{\kappa_{c(\tau)}}}\mathbf{F}^T_{\kappa_{c(\tau)}}\frac{d\alpha}{d\tau}d\tau\right],
\end{aligned} \tag{69}$$

and the entropy and Helmholtz potential are related through

$$\frac{\partial \psi}{\partial \theta} = -\eta. \tag{70}$$

We also note that for a Helmholtz potential consistent with that of an orthotropic elastic solid with ψ_c given by Eq. (60), we obtain the following representation

$$\begin{aligned}\mathbf{F}_{\kappa_{c(\tau)}} \frac{\partial \psi_c}{\partial \mathbf{C}_{\kappa_{c(\tau)}}} \mathbf{F}^T_{\kappa_{c(\tau)}} = \frac{\partial \psi_c}{\partial I_1} \mathbf{B}_{\kappa_{c(\tau)}} - \frac{\partial \psi_c}{\partial I_2} \mathbf{B}^{-1}_{\kappa_{c(\tau)}} + \mathbf{F}_{\kappa_{c(\tau)}} \Bigg(\frac{\partial \psi_c}{\partial J_1} \mathbf{n}_{\kappa_{c(\tau)}} \otimes \mathbf{n}_{\kappa_{c(\tau)}} + \\ \frac{\partial \psi_c}{\partial K_1} \mathbf{m}_{\kappa_{c(\tau)}} \otimes \mathbf{m}_{\kappa_{c(\tau)}} + \frac{\partial \psi_c}{\partial J_2} \Big(\mathbf{n}_{\kappa_{c(\tau)}} \otimes \mathbf{C}_{\kappa_{c(\tau)}} \mathbf{n}_{\kappa_{c(\tau)}} + \mathbf{C}_{\kappa_{c(\tau)}} \mathbf{n}_{\kappa_{c(\tau)}} \otimes \mathbf{n}_{\kappa_{c(\tau)}} \Big) + \\ \frac{\partial \psi_c}{\partial K_2} \Big(\mathbf{m}_{\kappa_{c(\tau)}} \otimes \mathbf{C}_{\kappa_{c(\tau)}} \mathbf{m}_{\kappa_{c(\tau)}} + \mathbf{C}_{\kappa_{c(\tau)}} \mathbf{m}_{\kappa_{c(\tau)}} \otimes \mathbf{m}_{\kappa_{c(\tau)}} \Big) \Bigg) \mathbf{F}^T_{\kappa_{c(\tau)}}. \end{aligned} \tag{71}$$

We define the partial stress in the amorphous phase through

$$\mathbf{T}_{a_i} = 2(1-\alpha)\rho \left[\frac{\partial \psi_a}{\partial I_i} \mathbf{B}_{\kappa_{p_i(t)}} + 2 \frac{\partial \psi_a}{\partial II_i} \mathbf{B}_{\kappa_{p_i(t)}} \right], i = 1, \ldots n. \tag{72}$$

Using Eq. (69), Eq. (70) and Eq. (72) in Eq. (68) we obtain

$$\sum_{i=1}^{n} \mathbf{T}_{a_i} \cdot \mathbf{D}_{\kappa_{p_i(t)}} + \rho \left(\psi_a - \psi_c \Big|_{\mathbf{C}_{\kappa_{c(t)}} = \mathbf{I}} - \frac{\partial i_\psi}{\partial \alpha} \right) \dot{\alpha} = \zeta_\alpha + \zeta_p. \tag{73}$$

For the forms selected for ψ_a, ψ_c, ζ_a and ζ_p it is clear that the following relationships hold,

$$\sum_{i=1}^{n} \mathbf{T}_{a_i} \cdot \mathbf{D}_{\kappa_{p_i(t)}} = \zeta_a, \tag{74}$$

$$\rho \left(\psi_a - \psi_c \Big|_{\mathbf{C}_{\kappa_{c(t)}} = \mathbf{I}} - \frac{\partial i_\psi}{\partial \alpha} \right) \dot{\alpha} = \zeta_p \tag{75}$$

Equation (74) places restrictions on the values that the tensors $\mathbf{D}_{\kappa_{p_i(t)}}$, $i = 1, .., n$ can take. At this stage we invoke the assumption of maximization of dissipation to determine the values of $\mathbf{D}_{\kappa_{p_i(t)}}$, $i = 1, .., n$, and $\dot{\alpha}$ that are allowable. Stated differently we choose values of $\mathbf{D}_{\kappa_{p_i(t)}}$ $i = 1, .., n$, that maximizes ζ_a satisfying the constraints given by Eq. (74) and Eq. (21) and we choose $\dot{\alpha}$ such that ζ_p is maximized subject to the constraint given by Eq. (75). Maximizing subject to the above mentioned constraints we obtain the following equations

$$\mathbf{T}_{a_i} - \beta_{1i} \frac{\partial \zeta_a}{\partial \mathbf{D}_{\kappa_{p_i(t)}}} - \beta_{2i} \mathbf{I} = \mathbf{0}, i = 1, \ldots, n, \tag{76}$$

where β_{1i} and β_{2i} are Lagrange multipliers associated with the constraints that are enforced. At this stage we need to prescribe the thermodynamic functions in order to proceed further with the derivation of an equation for $\mathbf{D}_{\kappa_{p_i(t)}}$. For the internal energy and entropy of the amorphous phase we use the same forms as the ones used in the melt region, i.e., Eq. (41) and Eq. (42) respectively. For crystalline materials there is not a significant change in the configurational entropy with deformation while the internal energy does depend on the deformation, because of which, we assume the following forms the internal energy and entropy of the crystalline phase,

$$\varepsilon_c = \varepsilon_c(\theta, I_C, II_C, J_1, J_2, K_1, K_2), \tag{77}$$

$$\eta_c = \eta_c(\theta). \tag{78}$$

We further assume that the internal energy can be split into a part that depends on the temperature and a part that depends on the deformation.

$$\varepsilon_c = \hat{\varepsilon}_c(\theta) + \tilde{\varepsilon}_c(I_C, II_C, J_1, J_2, K_1, K_2), \tag{79}$$

and we use a simple polynomial form for the dependence of the internal energy on the kinematical variables, consistent with that of a orthotropic elastic solid. The specific form chosen is

$$\varepsilon_c = \hat{\varepsilon}_c(\theta) + \frac{1}{2\rho}(\mu_c(I_C - 3) + \mu_{c_1}(J_1 - 1)^2 + \mu_{c_2}(K_1 - 1)^2), \tag{80}$$

where μ_c, μ_{c_1} and μ_{c_2} are material moduli associated with the crystalline phase. In addition, if the thermal component of the internal energy can be represented as a linear function of the temperature in the temperature interval of interest the internal energy takes the form:

$$\varepsilon_c = C_c\theta + A_c + \frac{1}{2\rho}(\mu_c(I_C - 3) + \mu_{c_1}(J_1 - 1)^2 + \mu_{c_2}(K_1 - 1)^2), \tag{81}$$

where C_c is the specific heat associated with the crystalline phase and A_c is a constant. In general these material moduli can depend on the deformation in the amorphous phase at the instant of crystallization through the tensors $\mathbf{B}_{\kappa_{p_i(t)}}$ $i = 1, \ldots n$. The entropy for the crystalline phase is given by

$$\eta_c = C_c \ln(\theta) + B_c, \tag{82}$$

where B_c is a constant. With the specification of these thermodynamic functions the Helmholtz potential for the mixture is completely specified and is obtained by substituting Eq. (41), Eq. (42) , Eq. (81) and Eq. (82) into Eq. (63) . The stress

tensor for the mixture is given by substituting the Helmholtz potential into Eq. (69) and using Eq. (71) to obtain:

$$\mathbf{T} = -p\mathbf{I} + \sum_{i=1}^{n}(1-\alpha)\Big(\mu_i \mathbf{B}_{\kappa_{p_i(t)}}\Big) + \int_{\tau_s}^{t} \mu_c \mathbf{B}_{\kappa_{c(\tau)}} \frac{d\alpha}{d\tau} d\tau +$$

$$2\int_{\tau_s}^{t}\Big(\mathbf{F}_{\kappa_{c(\tau)}}\Big(\mu_{c1}(J_1-1)\mathbf{n}_{\kappa_{c(\tau)}} \otimes \mathbf{n}_{\kappa_{c(\tau)}} + (\mu_{c_2}(K_1-1)\mathbf{m}_{\kappa_{c(\tau)}} \otimes \mathbf{m}_{\kappa_{c(\tau)}}\Big)\mathbf{F}^T_{\kappa_{c(\tau)}}\Big)\frac{d\alpha}{d\tau}d\tau. \tag{83}$$

The form for $\mathbf{T}_{a_i}$ is obtained from Eq. (72) as

$$\mathbf{T}_{a_i} = (1-\alpha)\mu_i \mathbf{B}_{\kappa_{p_i(t)}}. \tag{84}$$

The rate of dissipation in the amorphous part of the amorphous-crystalline mixture due to viscous effects, ζ_a, is assumed to be

$$\zeta_a = \sum_{i=1}^{n}(1-\alpha)2\nu_i \mathbf{D}_{\kappa_{p_i(t)}} \cdot \mathbf{B}_{\kappa_{p_i(t)}} \mathbf{D}_{\kappa_{p_i(t)}}. \tag{85}$$

This form is different from Eq. (45) for a purely amorphous melt in that the rate of dissipation is proportional to the amount of amorphous material remaining. Also, the formation of a crystalline phase affects the mobility of the molecules in the amorphous phase as the molecules are pinned down due to the crystalline phase. This manifests itself at the macroscopic level as an increase in the relaxation time of the amorphous phase. We incorporate this into the model by making the viscosity of the amorphous phase a function of the crystallinity, i.e.,

$$\nu_i = \nu_i(\theta, \alpha, \mathbf{B}_{\kappa_{p_i(t)}}), i = 1, \ldots, n. \tag{86}$$

Now, using the form for given ζ_a by Eq. (85) and utilizing Eq. (84) and Eq. (76) we obtain equations for $\mathbf{D}_{\kappa_{p_i(t)}}$, $i = 1, \ldots, n$, which are identical to Eq. (48) except for the viscosity which is given by Eq. (86) and depends on the crystallinity. In a manner identical to that used for the melt, from Eq. (48), we obtain rate equations for $\mathbf{B}_{\kappa_{p_i(t)}}$, $i = 1, \ldots, n$:

$$\overset{\nabla}{\mathbf{B}}_{\kappa_{p_i(t)}} := \dot{\mathbf{B}}_{\kappa_{p_i(t)}} - \mathbf{L}\mathbf{B}_{\kappa_{p_i(t)}} - \mathbf{B}_{\kappa_{p_i(t)}}\mathbf{L}^T = \frac{\mu_i}{\nu_i}\left(\frac{3}{\mathrm{tr}(\mathbf{B}^{-1}_{\kappa_{p_i(t)}})}\mathbf{I} - \mathbf{B}_{\kappa_{p_i(t)}}\right), \; i = 1, \ldots, n. \tag{87}$$

Note, Eq. (87) is identical to Eq. (49) with the exception that the viscosity is now given by Eq. (86) and is a function of crystallinity. This completes the specification

of an evolution equation for the natural configuration of the amorphous part in the mixture region.

The internal energy for the mixture is given by Eq. (61) with ε_a and ε_c given by Eq. (37) and Eq. (77) respectively. The energy equation for the mixture is derived by substituting the internal energy into the energy equation, Eq. (8), and using Eq. (69) and Eq. (71),

$$\rho\left(\alpha\frac{\partial\varepsilon_c}{\partial\theta}+(1-\alpha)\frac{\partial\varepsilon_c}{\partial\theta}\right)\dot{\theta}+\operatorname{div}\mathbf{q}=\sum_{i=1}^{n}\mathbf{T}_{a_i}\cdot\mathbf{L}+\rho\left(\varepsilon_a-\varepsilon_c-\frac{\partial i_\varepsilon}{\partial\alpha}\right)\dot{\alpha}+\rho r. \quad (88)$$

The above equation can be further simplified by substituting the specific forms for the internal energies given by Eq. (41), Eq. (81) and $\mathbf{T}_{a_i}$, $i=1,\ldots,n$ given by Eq. (84) to obtain:

$$\begin{aligned}\rho(\alpha C_c+(1-\alpha)C_a)+\operatorname{div}\mathbf{q}=&\sum_{i=1}^{n}(1-\alpha)\mu\mathbf{B}_{\kappa_{p_i(t)}}\cdot\mathbf{L}+\\ &\rho\left(C_a\theta+A_a-C_c\theta-A_c-\frac{\partial i_\varepsilon}{\partial\alpha}\right)\dot{\alpha}+\rho r.\end{aligned} \quad (89)$$

This completes the development of the equations for the mixture region. In the following sections we shall look more closely at the activation criterion indicating the onset of crystallization and the derivation of an equation for the rate at which crystallization takes place.

Initiation criterion

The initiation criterion for crystallization and the crystallization rate or the growth criterion are crucial ingredients that go into a crystallization model. The initiation criterion indicates the conditions in the melt at which crystallization begins while the growth criterion is an equation which gives the amount of material converted into the crystalline phase. We use Eq. (75) to derive both these equations. Note, in Eq. (75) the term in the brackets on the left hand side is the difference between the Helmholtz potential of the amorphous phase and the crystalline phase and this term acts as the driving force for crystallization. In the absence of this driving force crystallization will not take place. We define,

$$D_f:=\left(\psi_a-\psi_c\Big|_{\mathbf{C}_{\kappa_{c(t)}}=\mathbf{I}}-\frac{\partial i_\psi}{\partial\alpha}\right), \quad (90)$$

where D_f is defined to be the driving force behind the phase transition. This is analogous to the stress in Eq. (74) which acts the driving force to change the natural configuration of the amorphous phase.

When crystallization is initiated the crystallinity is identically zero and the driving force is given by

$$D_f\Big|_{\alpha=0} := \left(\psi_a - \psi_c\Big|_{\mathbf{C}_{\kappa_{c(t)}}=\mathbf{I}} - \frac{\partial i_\psi}{\partial \alpha}\Big|_{\alpha=0}\right). \tag{91}$$

We define the activation function through the driving force as

$$\phi\left(\theta, \mathbf{B}_{\kappa_{p_1(t)}}, \mathbf{B}_{\kappa_{p_2(t)}}, \ldots, \mathbf{B}_{\kappa_{p_n(t)}}\right) = D_f\Big|_{\alpha=0} - A, \tag{92}$$

where A is the initiation barrier and is a positive constant. Note that because of the forms chosen for ψ_a and ψ_c together with the assumption that the crystalline material is born in a stress free state the activation criterion depends on the temperature, θ, and the tensors $\mathbf{B}_{\kappa_{p_i(t)}}$, $i = 1, 2 \ldots n$. Crystallization cannot take place for negative values of the activation function as the driving force has not exceeded the initiation barrier, i.e.,

$$\phi\left(\theta, \mathbf{B}_{\kappa_{p_1(t)}}, \mathbf{B}_{\kappa_{p_2(t)}}, \ldots, \mathbf{B}_{\kappa_{p_n(t)}}\right) < 0 \Rightarrow \dot{\alpha} = 0, \tag{93}$$

When the temperature, θ, and $\mathbf{B}_{\kappa_{p_i(t)}}$, $i = 1, 2 \ldots n$, at a material point are such that

$$\phi\left(\theta, \mathbf{B}_{\kappa_{p_1(t)}}, \mathbf{B}_{\kappa_{p_2(t)}}, \ldots, \mathbf{B}_{\kappa_{p_n(t)}}\right) = 0, \tag{94}$$

crystallization is about to begin and that particular material point is on the activation surface. Now if θ, and $\mathbf{B}_{\kappa_{p_i(t)}}$, $i = 1, 2 \ldots n$, are varied such that the value of ϕ decreases, crystallization will not be initiated. If, however θ, and $\mathbf{B}_{\kappa_{p_i(t)}}$, $i = 1, 2 \ldots n$ are varied such that ϕ increases and exceeds zero, crystallization is initiated. The activation criterion for the initiation of crystallization can be stated more precisely as follows:

$$\begin{gathered}\phi\left(\theta, \mathbf{B}_{\kappa_{p_1(t)}}, \mathbf{B}_{\kappa_{p_2(t)}}, \ldots, \mathbf{B}_{\kappa_{p_n(t)}}\right) > 0 \text{ or} \\ \phi\left(\theta, \mathbf{B}_{\kappa_{p_1(t)}}, \mathbf{B}_{\kappa_{p_2(t)}}, \ldots, \mathbf{B}_{\kappa_{p_n(t)}}\right) = 0, \quad \frac{\partial \phi}{\partial \theta}\dot{\theta} + \sum_{i=1}^{n} \frac{\partial \phi}{\partial \mathbf{B}_{\kappa_{p_i(t)}}} \cdot \dot{\mathbf{B}}_{\kappa_{p_i(t)}} > 0.\end{gathered} \tag{95}$$

The above equation is similar to the strain space loading criterion in plasticity (see [48]). This completes the specification of the initiation criterion. In the next section we shall outline the methodology used to derive the crystallization rate.

Crystallization rate

In the literature devoted to polymer physics, crystallization kinetics are usually studied using an Avrami type approach which is based on the notion of filling space through the nucleation and growth of one phase into another. In this approach it is assumed that nucleation is initiated at certain locations known as nucleation sites. After the nucleation has taken place the growth of the crystalline material at these nucleation sites is prescribed by a growth rate. The nucleation rate and the growth rate are usually prescribed as functions of time. With these two inputs it is possible to derive equations governing the crystallization kinetics. The Avrami approach has however some significant draw backs. In such a theory there is no notion of an activation criterion, making it difficult to apply the equation to problems where the exact instant when crystallization is initiated is not known. This is specially true of non-isothermal problems. Another drawback is the lack of connection with the thermodynamic quantities in the problems such as the internal energy and entropy. Due to this, the deformation of the melt, which influences the entropy of the melt, cannot be introduced into the theory in a consistent manner. Also, there are certain polymers such as polyethylene terephthalate which at temperatures just above the glass transition temperature crystallize only due to deformation. The kinetics of such crystallization does not follow the behavior predicted by the Avrami equation, hence it is not general enough to capture the various types of crystallization behavior observed in polymers. For these reasons we do not pursue this approach here (more information on the Avrami approach can be found in [43], [77] and [15]).

After the initiation of crystallization we use the assumption of maximization of dissipation along with Eq. (75) to determine an equation for the amount of crystalline material formed. Re-writing Eq. (75) and using Eq. (90) we obtain

$$\rho D_f \dot{\alpha} = \zeta_p. \tag{96}$$

The equation for the crystallization rate, $\dot{\alpha}$, is obtained by solving Eq. (96) for $\dot{\alpha}$. As Eq. (96) is in general nonlinear, more than one value of $\dot{\alpha}$ are possible. The value of $\dot{\alpha}$ chosen is the one that maximizes the rate of dissipation. The exact form for the rate of crystallization depends on the specific form chosen for ζ_p, the choice of which depends on the specific polymer being modeled. The rate of dissipation due to crystallization, ζ_p, is expected to depend on the crystallinity, α, the rate of change of crystallinity, $\dot{\alpha}$, and in general it can also depend on other variables like temperature and other kinematical variables as well, i.e.,

$$\zeta_p = \zeta_p(\alpha, \dot{\alpha}, \theta, \mathbf{B}_{\kappa_{p_1(t)}}, \mathbf{B}_{\kappa_{p_2(t)}}, \ldots \mathbf{B}_{\kappa_{p_n(t)}}). \tag{97}$$

Note, ζ_p has to be exactly zero when no crystallization is taking place, this can be written as

$$\zeta_p\Big|_{\dot{\alpha}=0} = 0. \tag{98}$$

To derive the specific rate equations for crystallization, we need to prescribe a form for the rate of dissipation. We shall derive a specific rate equation for $\dot{\alpha}$ when we formulate a model and apply it to bi-axial extension. Here it should be noted that the Avrami equation can be directly obtained by choosing appropriate forms for the rate of dissipation.

Transition to solid-like behavior

The transition to solid-like behavior takes place when the mobility of the molecules in the amorphous phase decreases. This can happen because of a drop in the temperature or if the amount of crystalline phase is sufficiently high to pin down the motion of the molecules. The amount of material crystallized is determined form the rate equation derived from Eq. (96). The amount of crystalline material formed and the temperature have a bearing on the behavior of the amorphous phase. The viscosity of the amorphous phase is a function of both the temperature and crystallinity, with the viscosity increasing with an increase in crystallinity and also increasing with a decrease in temperature. Consequently the relaxation time, given by Eq. (50) also increases with an increase in crystallinity and a decrease in the temperature.

The amorphous phase has been modeled as a viscoelastic fluid. These fluid models transition to that of an elastic solid for large values of relaxation time (or large values of viscosity for finite values of the shear modulus). This is evident from Eq. (87), as $\nu_i \to \infty$ for finite values of μ_i, Eq. (87) reduces to

$$\overset{\nabla}{\mathbf{B}}_{\kappa_{p_i(t)}} := \dot{\mathbf{B}}_{\kappa_{p_i(t)}} - \mathbf{L}\mathbf{B}_{\kappa_{p_i(t)}} - \mathbf{B}_{\kappa_{p_i(t)}}\mathbf{L}^T = \mathbf{0}, \quad , i = 1, 2 \ldots n. \tag{99}$$

The above equation is also obtained by taking the material time derivative of the tensors $\mathbf{B}_{\kappa_{p_i(t)}}$, $i = 1, 2 \ldots n$, keeping the reference configuration fixed, which is the case for an elastic solid. The underlying natural configurations of the amorphous phase do not evolve and the response of the amorphous material is that of a mixture of isotropic elastic solids, the specific model is given by the form chosen for the Helmholtz potential, i.e., by the elastic response embedded in the viscoelastic fluid model. It is important to note that increasing the viscosity in a Newtonian fluid does not give a solid model but only a fluid with a large viscosity and thus doing so is an inaccurate way to model the transition from a fluid like behavior to a solid like behavior. Also, not all viscoelastic fluid models will transition to an elastic solid model for large values of relaxation time. After the transition to a solid is

complete the stress is given by

$$\mathbf{T} = -p\mathbf{I} + \sum_{i=1}^{n} 2(1-\alpha_0)\rho \left[\frac{\partial \psi_a}{\partial I_i} \mathbf{B}_{\kappa_{p_i(t)}} + 2\frac{\partial \psi_a}{\partial II_i} \mathbf{B}^2_{\kappa_{p_i(t)}} \right] + 2\rho \left[\int_{\tau_s}^{\tau_e} \mathbf{F}_{\kappa_{c(t)}} \frac{\partial \psi_c}{\partial \mathbf{C}_{\kappa_{c(t)}}} \mathbf{F}^T_{\kappa_{c(t)}} \frac{d\alpha}{d\tau} d\tau \right], \tag{100}$$

where α_0 is the final crystallinity in the material and τ_e is the time at which crystallization ended. The final behavior of the semi-crystalline material is that of a mixture of an isotropic elastic solid and an anisotropic elastic solid. The energy equation for the solid with internal energies of the amorphous and crystalline phases given by Eq. (37) and Eq. (77) is

$$\rho \left(\alpha \frac{\partial \varepsilon_c}{\partial \theta} + (1-\alpha) \frac{\partial \varepsilon_a}{\partial \theta} \right) \dot{\theta} + \operatorname{div} \mathbf{q} = \sum_{i=1}^{n} \mathbf{T}_{a_i} \cdot \mathbf{L} + \rho r. \tag{101}$$

With the specific forms for the internal energies given by Eq. (41) and Eq. (81) and $\mathbf{T}_{a_i}$ given by Eq. (84), the energy equation reduces to

$$\rho(\alpha C_c + (1-\alpha) C_a)\dot{\theta} + \operatorname{div} \mathbf{q} = \sum_{i=1}^{n} (1-\alpha)\mu_i \mathbf{B}_{\kappa_{p_i(t)}} \cdot \mathbf{L} + \rho r. \tag{102}$$

Equation (88) is different from Eq. (89) as crystallization has ceased and thus the contribution due to the latent energy term is zero. This completes the development of the equations to describe the process of crystallization.

Application of the model to bi-axial extension

In this section we illustrate the application of the model to bi-axial extension. First we develop a simplified model containing all the main features of crystallization and apply it to a problem of bi-axial extension. For the model used in this calculation we assume that the amorphous phase has a single relaxation time, i.e., a single natural configuration associated with it. For this case the stress in the melt is given by

$$\mathbf{T} = -p\mathbf{I} + \mu \mathbf{B}_{\kappa_{p(t)}}, \tag{103}$$

note that since there is a single relaxation mechanism, we do not use the subscript i as in Eq. (43). The evolution of the natural configuration is given by

$$\overset{\triangledown}{\mathbf{B}}_{\kappa_{p(t)}} := \dot{\mathbf{B}}_{\kappa_{p(t)}} - \mathbf{L}\mathbf{B}_{\kappa_{p(t)}} - \mathbf{B}_{\kappa_{p(t)}}\mathbf{L}^T = \frac{\mu}{\nu} \left(\frac{3}{\operatorname{tr}(\mathbf{B}_{\kappa_{p(t)}})} \mathbf{I} - \mathbf{B}_{\kappa_{p(t)}} \right), \tag{104}$$

where the viscosity, ν, for polymer melts is commonly described through the following relationship (see [40])

$$\nu = \nu_0 \exp\left(L_\theta \left(\frac{1}{\theta} - \frac{1}{\theta_R}\right)\right). \tag{105}$$

In the above equation, ν_0 is the viscosity at a given reference temperature, θ_R, and L_θ is a constant. The energy equation is given by Eq. (52), and in this example we neglect the effect of radiant heating. After the onset of crystallization the stress tensor takes the form

$$\mathbf{T} = -p\mathbf{I} + (1-\alpha)(\mu \mathbf{B}_{\kappa_{p(t)}}) + \int_{\tau_s}^{t} \mu_c \mathbf{B}_{\kappa_{c(\tau)}} \frac{d\alpha}{d\tau} d\tau +$$

$$2\int_{\tau_s}^{t} \left(\mathbf{F}_{\kappa_{c(\tau)}} \left(\mu_{c1}(J_1 - 1)\mathbf{n}_{\kappa_{c(\tau)}} \otimes \mathbf{n}_{\kappa_{c(\tau)}} + \mu_{c_2}(K_2 - 1)\mathbf{m}_{\kappa_{c(\tau)}} \otimes \mathbf{m}_{\kappa_{c(\tau)}}\right) \mathbf{F}^T_{\kappa_{c(\tau)}}\right) \frac{d\alpha}{d\tau} d\tau. \tag{106}$$

The unit vectors $\mathbf{n}_{\kappa_{c(\tau)}}$ and $\mathbf{m}_{\kappa_{c(\tau)}}$ depend on the directions of stretch in the amorphous phase through the eigenvalues of $\mathbf{B}_{\kappa_{p(\tau)}}$ at the instant at which the crystals were formed, as has been described in the earlier sections. The equation for the evolution of the natural configuration of the amorphous phase after the onset of crystallization is given by Eq. (104), except that the viscosity is now a function of both the temperature and crystallinity and is given by

$$\nu = \nu_0 \exp\left(L_\theta \left(\frac{1}{\theta} - \frac{1}{\theta_R}\right)\right) \exp(L_\alpha \alpha), \tag{107}$$

where L_α is a constant. This dependence of the viscosity on the temperature and crystallinity is similar to the form used in [29]. The energy equation for the mixture is given by Eq. (89). The activation function, ϕ, takes the form

$$\phi(\theta, \mathbf{B}_{\kappa_{p(t)}}) = \left(\frac{\theta_m^0 - \theta}{\theta_m^0}\right) - \frac{1}{\Delta H_f} \frac{\partial i_\psi}{\partial \alpha}\bigg|_{\alpha=0} + \frac{\mu(\mathrm{tr}(\mathbf{B}_{\kappa_{p(t)}}) - 3)}{2\rho \Delta H_f}, \tag{108}$$

where ΔH_f is the latent heat. Note, in the above equation the latent energy near the vicinity of the equilibrium melting temperature has been derived assuming that the energy and entropy of the two phases are independent in this temperature range (see [27]). To derive an equation for the rate of crystallization, we need to prescribe a form for the rate of dissipation due to crystallization. The form chosen for this example is

$$\zeta_p = \frac{\dot{\alpha}^m}{\bar{G}(\alpha_0 - \alpha)^k}, \tag{109}$$

where the constant α_0 represents the maximum crystallinity and $\bar{G}$, k and m are constants. Note when the crystallinity approaches α_0 the rate of dissipation becomes very large effectively curtailing any further crystallization. In addition the form chosen for ζ_p satisfies the condition described by Eq. (98). For this choice for the rate of dissipation the rate of crystallization takes the form

$$\dot{\alpha} = G(\alpha_0 - \alpha)^{k/m-1} \left(\left(\frac{\theta_m^0 - \theta}{\theta_m^0} \right) - \frac{1}{\Delta H_f} \frac{\partial i_\psi}{\partial \alpha} + \frac{\mu(\mathrm{tr}(\mathbf{B}_{\kappa_{p(t)}}) - 3)}{2\rho \Delta H_f} \right)^{1/m-1}, \tag{110}$$

where G is a constant. At the end of crystallization the stress in the mixture is given by Eq. (106) with upper limit of the integral replaced by τ_e.

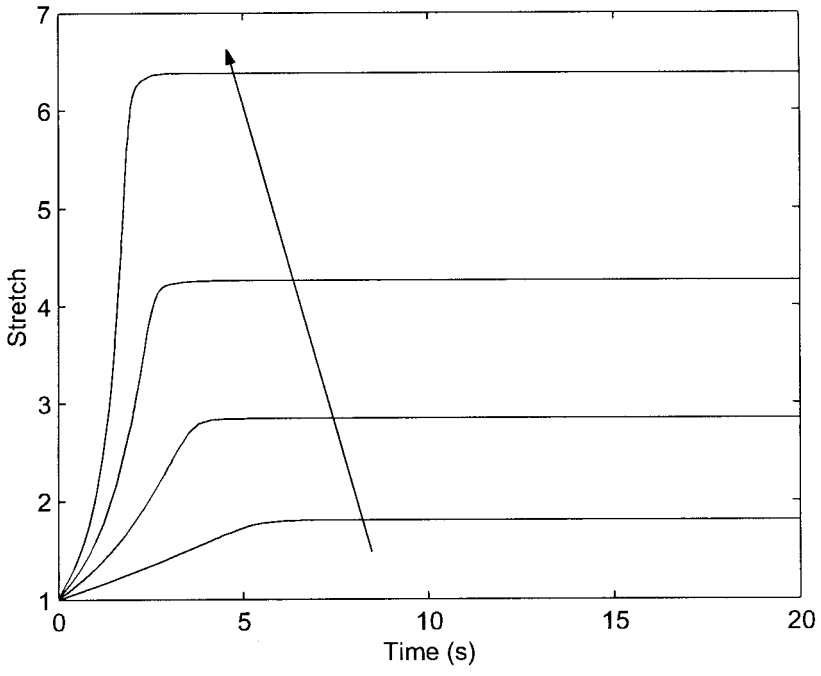

Figure 3. Stretch vs. time for $T_{11}^{(0)}/\mu = 0.05, 0.1, 0.15, 0.2$.

The film is stretched by subjecting it to a constant force in two perpendicular directions (say the x and y direction) while the third surface is traction free. In addition, the film also loses thermal energy to its environment, the magnitude of which is determined by a prescribed heat transfer coefficient. The initial temperature of the film is above the crystallization temperature in these calculations, we

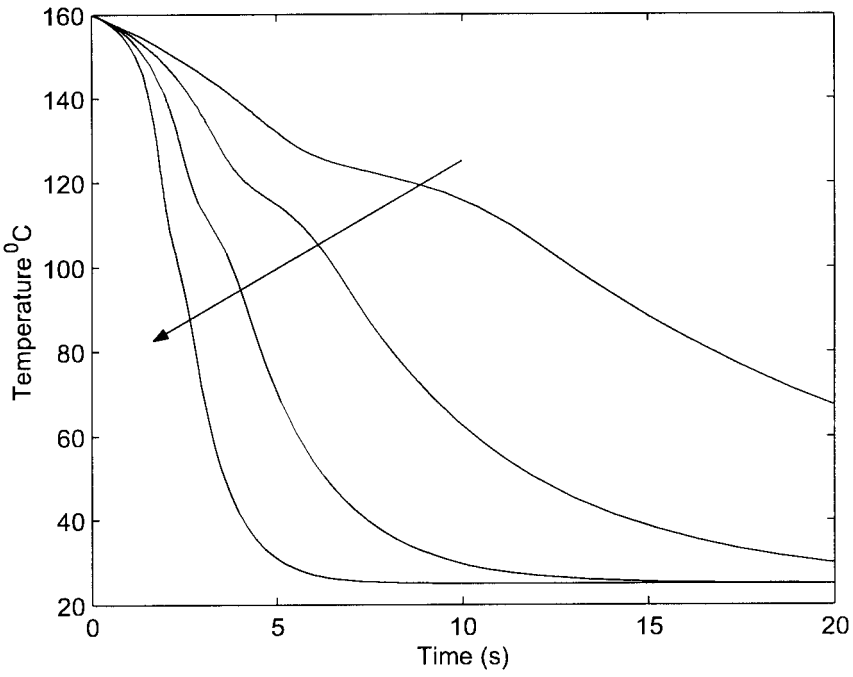

Figure 4. Temperature vs. time for $T_{11}^{(0)}/\mu = 0.05, 0.1, 0.15, 0.2$.

take it to be 160°C, therefore the film is initially an amorphous melt. As the film cools and is simultaneously being deformed, crystallization is initiated. This problem is similar to what is commonly encountered in film blowing and film stretching applications wherein the film is simultaneously being cooled and stretched during crystallization. In both these processes, the film is stretched in two perpendicular directions while being cooled. The kinematics for homogenous bi-axial extension is given by

$$x = \Lambda(t)X, \quad y = \Lambda(t)Y, \quad z = \frac{Z}{\Lambda(t)^2}, \tag{111}$$

where X, Y, Z are the co-ordinates in undeformed configuration, x, y, z are the co-ordinates in the deformed configuration and $\Lambda(t)$ is the stretch. The velocity gradient is given by

$$\mathbf{L} = \operatorname{diag}\left(\frac{\dot{\Lambda}}{\Lambda}, \frac{\dot{\Lambda}}{\Lambda}, -2\frac{\dot{\Lambda}}{\Lambda}\right). \tag{112}$$

The other kinematical tensors, namely $\mathbf{B}_{\kappa_{p(t)}}$, $\mathbf{F}_{\kappa_{c(\tau)}}$, $\mathbf{C}_{\kappa_{c(\tau)}}$ are also diagonal.

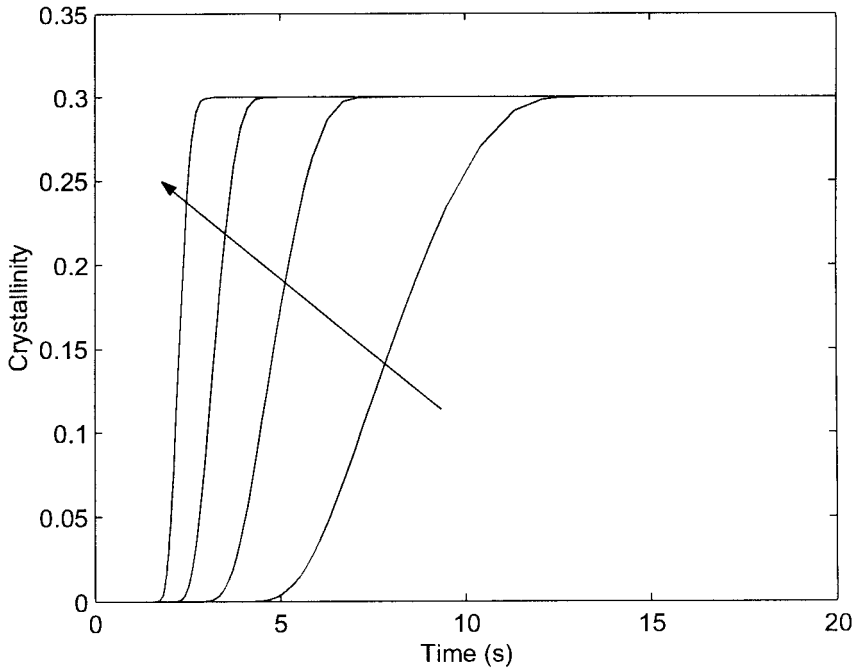

Figure 5. Crystallinity vs. time for $T_{11}^{(0)}/\mu = 0.05, 0.1, 0.15, 0.2$.

The tensors $\mathbf{F}_{\kappa_{c(\tau)}}$ and $\mathbf{C}_{\kappa_{c(\tau)}}$ are given by

$$\mathbf{F}_{\kappa_{c(\tau)}} = \operatorname{diag}\left(\frac{\Lambda(t)}{\Lambda(\tau)}, \frac{\Lambda(t)}{\Lambda(\tau)}, \left(\frac{\Lambda(\tau)}{\Lambda(t)}\right)^2\right), \tag{113}$$

$$\mathbf{C}_{\kappa_{c(\tau)}} = \operatorname{diag}\left(\left(\frac{\Lambda(t)}{\Lambda(\tau)}\right)^2, \left(\frac{\Lambda(t)}{\Lambda(\tau)}\right)^2, \left(\frac{\Lambda(\tau)}{\Lambda(t)}\right)^4\right). \tag{114}$$

Since the film is stretched equally in two perpendicular directions, we need consider the stress in any one of the two directions, here we consider the x direction. As the film is stretched by the application of a constant force, ignoring inertial effects, the stress is given by

$$T_{11}^{(0)} = \frac{F}{wh} = \frac{T_{11}}{\Lambda}, \tag{115}$$

where $T_{11}^{(0)}$ is the stress per unit initial area, w is the initial width of the film perpendicular to the x direction and h is the initial thickness of the film and F

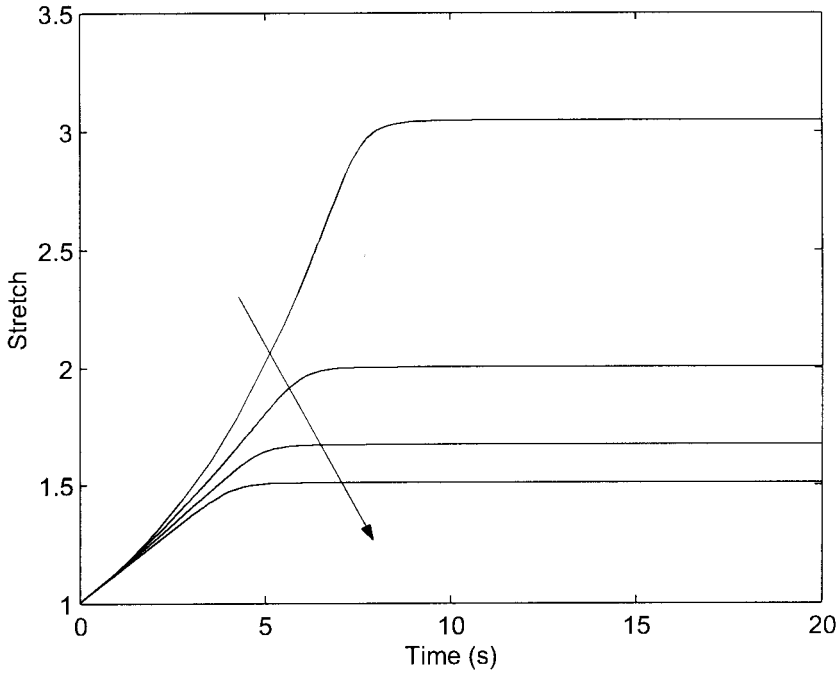

Figure 6. Stretch vs. time for $H/\rho Ch = .01, .02, .03, .04$.

is the applied force. Initial conditions on $\Lambda(t)$ are obtained by recognizing that initially the film is an amorphous melt (viscoelastic material) and on the sudden application of a force, it reacts instantaneously like an elastic solid. The initial value of $\Lambda(t)$, i.e., $\Lambda(0)$ is given as a solution to the following equation

$$T_{11} = T_{11}^{(0)}\Lambda(0) = \mu\left(\Lambda(0)^2 - \frac{1}{\Lambda(0)^4}\right). \tag{116}$$

The energy equation for this problem simplifies to

$$\frac{d\theta}{dt} = -\frac{H\Lambda^2}{\rho Ch}(\theta - \theta_a) + \frac{\Delta H_f}{C}\dot{\alpha} + \frac{\mu(1-\alpha)\mathbf{B}_{\kappa_{p(t)}} \cdot \mathbf{L}}{C}, \tag{117}$$

where C is an averaged value for the specific heat, H is the heat transfer coefficient and θ_a is the ambient temperature (in this work $\theta_a = 25°\text{C}$). Since our aim here is to illustrate the general behavior of the model for this calculation, we ignore the affects of the interfacial energy on the crystallization kinetics. The governing system of integro-differential equations (Eq. (104), Eq.(106), Eq.(110), Eq.(115)

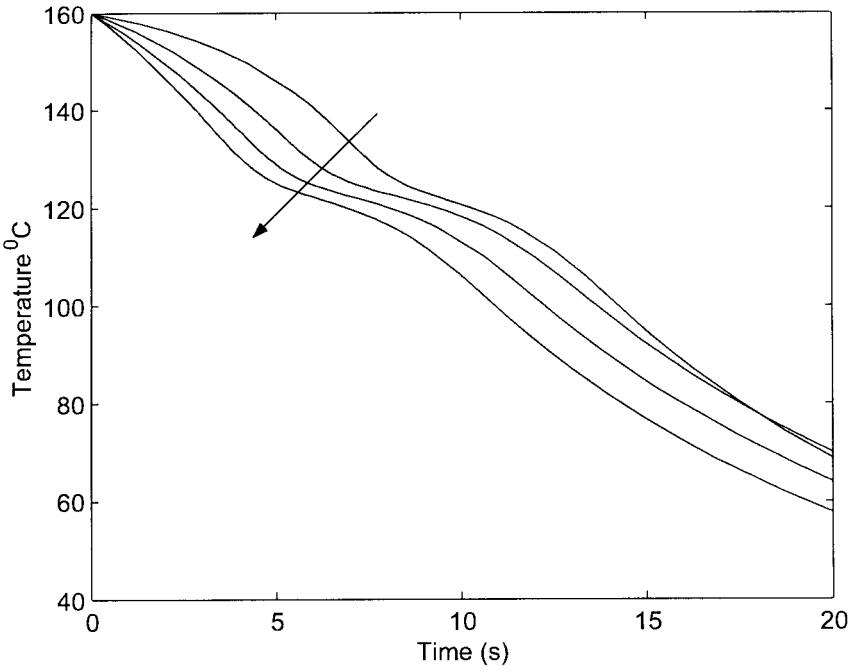

Figure 7. Temperature vs. time for $H/\rho Ch = .01, .02, .03, .04$.

and Eq. (117) are solved numerically. The material constants used are consistent with values for polyethylene: $C = 2.96\text{kJ/kg}^0\text{C}$, $\rho = 900\text{kg/m}^3$, $\theta_m^0 = 141°\text{C}$, $\Delta H_f = 275\text{kJ/kg}$, $\alpha_0 = 0.3$, $\mu = 2.0E + 5$ Pa, $\nu_0 = 2.0E + 5$ Pa-s, $\theta_R = 150°\text{C}$, $m = 4/3$, $n = 1/3$, $G = 4000\text{s}^{-1}$ $L_\theta = 5000$ ^{o}K, $L_\alpha = 30$, $\frac{\mu_c}{\mu} = 10$, $\frac{\mu_{c1}}{\mu} = 2$, $\frac{\mu_{c_2}}{\mu} = 2$. The initial thickness of the film, h, is taken to be 1 mm. The results are discussed in the next section.

Results and discussion

For the problem under consideration we present two sets of results. For the first set of results we vary the stretching force and observe its effect on the stretch, Λ, temperature, θ and crystallinity, α. For these calculations $H/\rho hC = 0.025\text{s}^{-1}$. A plot of the stretch versus time is shown in figure 3. When the material is subject to the stretching force it instantaneously acts like an elastic solid, therefore the stretch at time $t = 0$ is greater than unity. Initially, the stretch increases, until the temperature drops and crystallization begins. After the onset of crystallization, the film becomes stiffer, finally deformation ceases and the material becomes a

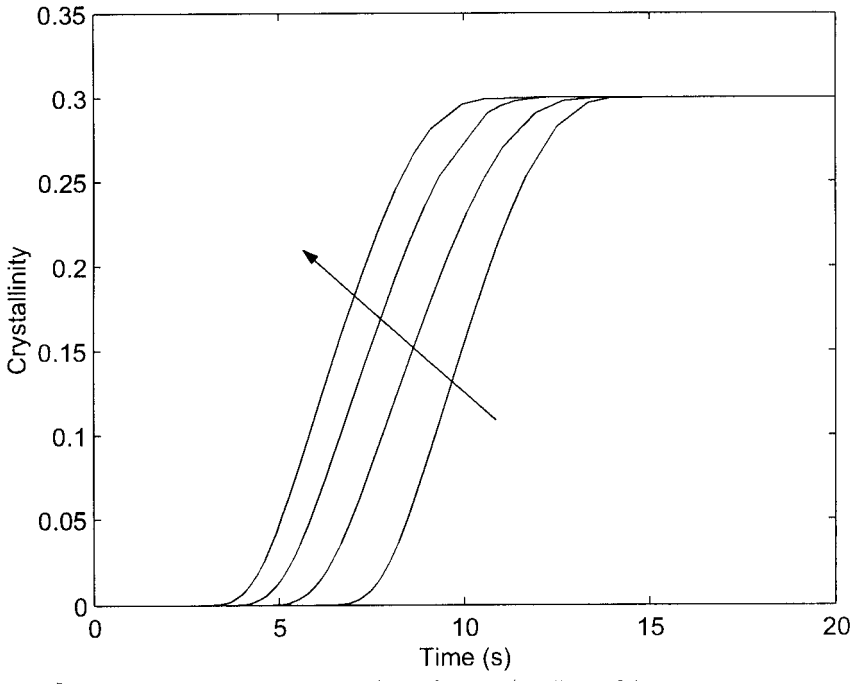

Figure 8. Crystallinity vs. time for $H/\rho Ch = .01, .02, .03, .04$.

solid. For higher loads, the value of the final stretch increases. A plot of the temperature versus time is shown in figure 4. The temperature decreases steadily until crystallization begins. After the onset of crystallization latent energy is released and the temperature profile exhibits a plateau associated with crystallization. After the completion of crystallization, the temperature continues to drop towards the ambient temperature. Figure 5 shows the evolution of crystallinity with time, for the four different cases. The crystallinity increases monotonically with time. We note that the plateau in the temperature curves, and the decrease in the rate of stretch coincide with the onset of crystallization. For higher stretching forces, the film stretches more rapidly, enhancing the heat transfer resulting in the earlier onset of crystallization. Figures 6, 7 and 8 present the stretch, temperature and crystallinity for four different cooling rates with $T_{11}^{(0)}/\mu = 0.05$. At higher cooling rates, crystallization is initiated earlier and the final stretch of the film is lower than the value for lower cooling rates. These results are consistent with what has been observed in the literature for film blowing and film stretching(see [28], [7]).

Summary

In this paper we have developed a general framework to construct models that can describe crystallization in polymers. The framework is general enough that models capable of describing the crystallization behavior of different polymers can be easily generated. Models applicable to specific polymers have been developed within this framework and have been used to solve different boundary value problems. The framework is built on the idea of evolving natural configurations and the maximization of the rate of dissipation. Specific models are constructed by specifying forms for the internal energy, entropy and rate of dissipation. The reduced energy-dissipation equation is used to obtain the constitutive relation for the stress and the maximization of the rate of dissipation is used to obtain equations for the evolution of the underlying natural configuration and the rate of crystallization. The behavior of the amorphous phase is described by the use of rate type models while the crystalline phase is described by the use of models consistent with those for an anisotropic elastic solid. The anisotropy in the mechanical behavior of the crystalline phase depends on the deformation in the amorphous phase at the instant of formation. The activation criterion that indicates the onset of crystallization is defined in terms of the driving force behind the phase transition, namely, the difference in the Helmholtz potential between the amorphous and crystalline phase. Finally, it should be noted that the exact mechanisms governing the details of polymer crystallization are still not well understood, the framework presented here is general enough that most specific details can be incorporated into the model in a direct way.

Acknowledgements

The authors thank the National Science Foundation and the Polymer Film Consortium at Texas A&M University for supporting this work. In addition, one of the authors (I. J. Rao) acknowledges the support provided by the New Jersey Institute of Technology under Grant No. 421060.

References

[1] R. J. Atkin and R. E. Craine, Continuum theory of mixtures: basic theory and historical development. *Quarterly Journal of Mechanics and Applied Mathematics*, **29** (1976), 209-244.

[2] M. Avrami, Kinetics of phase change. I. General theory. *Journal of Chemical Physics*, **7** (1939), 1103-1112.

[3] M. Avrami, Kinetics of phase change. II. Transformation-time relations for random distribution of nuclei. *Journal of Chemical Physics*, **8** (1940), 212-224.

[4] M. Avrami, Kinetics of phase change. III. Granulation, phase change, and microstructure. *Journal of Chemical Physics*, **9** (1941), 177-184.

[5] F. Baldoni and K.R. Rajagopal, A continuum theory for the thermomechanics of solidification. *International Journal of Non Linear Mechanics*, **32** (1997), 3-20.
[6] S. G. Bankoff, Heat conduction or diffusion with phase change. *Advances in Chemical Engineering*, **5** (1964), 75-150.
[7] G. L. Bourvellec and J. Beautemps, Stretching of PET films under constant load. 1. Kinetics and deformation. *Journal of Applied Polymer Science*, **39** (1990), 319-328.
[8] R. M. Bowen, *Theory of mixtures, in Continuum Physics*, Vol. III, A.C. Eringen, ed., Academic Press, New York 1975.
[9] A. C. Bushman and A. J. McHugh, A continuum model for the dynamics of flow induced crystallization. *Journal of Polymer Science: Part B: Polymer Physics*, **34** (1996), 2393-2407.
[10] J. Crank, *Free and Moving Boundary Problems*. Clarendon Press, Oxford 1984.
[11] Z. Ding and J.E. Spruiell, Interpretation of the nonisothermal crystallization kinetics of polypropylene using a power law nucleation rate function. *Journal of Polymer Science: Part B: Polymer Physics*, **35** (1997), 1077-1092.
[12] A. K. Doufas, A. J. McHugh, and C. Miller, Simulation of melt spinning including flow-induced crystallization. Part 1. Model development and predictions. *Journal of Non-Newtonian Fluid Mechanics*, **92** (2000), 27-66.
[13] C. Eckart, The thermodynamics of irreversible processes. IV. The theory of elasticity and anelasticity. *Physical Review*, **73** (1948), 373-382.
[14] G. Eder, H. Janeschitz-Kriegl, and G. Krobath, Shear induced crystallization, a relaxation phenomenon in melts. *Progress in Colloid and Polymer Science*, **80** (1989), 1-7.
[15] G. Eder, H. Janeschitz-Kriegl, and S. Liedauer, Crystallization processes in quiescent and moving polymer melts under heat transfer conditions. *Progress in Polymer Science*, **15** (1990), 629-714.
[16] A. Fasano and M. Primicerio, Free boundary problems for nonlinear equations with nonlinear free boundary conditions. *Journal of Mathematical Analysis and Applications*, **72** (1979), 247-273.
[17] P. J. Flory, Thermodynamics of crystallization in high polymers I. Crystallization induced by stretching. *Journal of Chemistry and Physics*, **15** (1947), 397-408.
[18] P. J. Flory, D. Y. Yoon, and K. A. Dill, The interphase in lamellar semicrystalline polymers. *Macromolecules*, **17** (1984), 862-868.
[19] R. J. Gaylord, A theory of stress induced crystallization of cross linked polymer networks. *Journal of Polymer Science.*, **14** (1976), 1827-1837.
[20] R. J. Gaylord and D. J. Lohse, Morphological changes during oriented polymer crystallization. *Polymer Engineering and Science*, **16** (1976), 163-167.
[21] M. E. Glicksman, S. R. Corriell, and G. B. McFadden, Interaction of flows with the crystal melt interface. *Annual Reviews in Fluid Mechanics*, **18** (1986), 307-335.
[22] A. E. Green and P. M. Naghdi, On thermodynamics and the nature of the second law. *Proceedings of the Royal Society, London, A*, **357** (1977), 253-270.
[23] T. W. Haas and B. Maxwell, Effects of shear stress on the crystallization of linear polyethylene and polybutene-1. *Polymer Engineering and Science*, **9** (1969), 225-241.
[24] R. N. Hills, D. E. Loper, and P. H. Roberts, A thermodynamically consistent model of a mushy zone. *Quarterly Journal of Mechanics and Applied Mathematics*, **36** (1983), 505-539.
[25] R. N. Hills and P. H. Roberts, On the formulation of a diffusive mixture theory for two-phase region. *Journal of Engineering Mathematics*, **22** (1988), 93-106.
[26] R. N. Hills and P. H. Roberts, A macroscopic modeling of phase coarsening. *International Journal of Non Linear Mechanics*, **25** (1990), 319-329.
[27] J. D. Hoffman and J. J. Weeks, Rate of spherulitic crystallization with chain folds in polychlorotrifluoroethylene. *Journal of Chemical Physics*, **37** (1962), 1723- 1741.
[28] T. Kanai and J. L. White, Kinematics, dynamics and stability of the tubular film extrusion

of various polyethylenes. *Polymer Engineering and Science*, **24** (1984), 1185-1201.

[29] T. Kanai and J. L. White, Dynamics, heat transfer and structure development in tubular film extrusion of polymer melts: a mathematical model and predictions. *Journal of Polymer Engineering*, **5** (1985), 135-157.

[30] K. Katayama, S. Murakami, and K. Kobayashi, An apparatus for measuring flow induced crystallization in polymers. *Bulletin of the Institute of Chemistry Research, Kyoto University*, **54** (1976), 82-90.

[31] T. Kawai, M. Iguchi, and H. Tonami, Crystallization of polyethylene under molecular orientation. *Kolloid-Zeitschrift and Zeitschrift für Polymere*, **221** (1967), 28-40.

[32] A. Keller and M. J. Machin, Direct evidence for distinctive, stress induced nucleus crystals in the crystallization of oriented polymer melts. *Journal of Macromolecular Science (Physics)*, **B3** (1969), 153-169.

[33] K. Kobayashi and T. Nagasawa, Crystallization of sheared polymer melts. *Journal of Macromolecular Science (Physics)*, **B4** (1970), 331-345.

[34] G. Kumaraswamy, A. M. Issaian, and J. A. Kornfield, Shear enhanced crystallization in isotactic polypropylene. 1. Correspondence between in situ rheo-optics and ex situ structure determination. *Macromolecules*, **32** (1999), 7537-7547.

[35] G. Kumaraswamy, R. K. Verma, A. M. Issaian, P. Wang, J. A. Kornfield, F. Yeh, B. S. Hsiao, and R. H. Olley, Shear enhanced crystallization in isotactic polypropylene. Part 2. Analysis of formation of oriented "skin". *Polymer*, **41** (2000), 8931-8940.

[36] K. Kuwabara, H. Kaji, F. Horii, D. C. Basset, and R. H. Olley, Solid-state 13C NMR analyses of the crystalline-noncrystalline structure for metallocene- catalyzed linear low-density polyethylene. *Macromolecules*, **30** (1997), 7516- 7521.

[37] R. R. Lagasse and B. Maxwell, An experimental study of the kinetics if polymer crystallization during shear flow. *Polymer Engineering and Science*, **16** (1976), 189-199.

[38] M. M. Lamé and B. P. E. Clapeyron, Memoire sur la solidification par refroidissement d'un globe liquide. *Annales Chimie Physique*, **47** (1831).

[39] L. D. Landau, *Collected Papers*. Gordon and Breach, New York 1967.

[40] A. I. Leonov and A. N. Prokunin, *Nonlinear Phenomena in Flows of Viscoelastic Polymer Fluids*. Chapman & Hall, New York 1994.

[41] M. R. Mackley and A. Keller, Flow induced crystallization in polyethylene melts. *Polymer*, **14** (1973), 16-20.

[42] M. R. Mackley, F. C. Frank, and A. Keller, Flow induced crystallization in polyethylene melts. *Journal of Materials Science*, **10** (1975), 1501-1509.

[43] L. Mandelkern, *Crystallization of Polymers*. McGraw Hill, New York 1964.

[44] L. Mandelkern, M. Glotin, and R. A. Benson, Supermolecular structure and thermodynamic properties of linear and branched polyethylenes under rapid crystallization conditions. *Macromolecules*, **14** (1981), 22-34.

[45] A. J. McHugh, R. K. Guy, and D.A . Tree, Extensional flow-induced crystallization of a polyethylene melt. *Colloids and Polymer Science*, **271** (1993), 629-645.

[46] A. J. McHugh, Flow induced crystallization in polymers., in *Rheo-physics of Multiphase Polymeric Systems*, J. Lyngaae-Jorgenson and K. Sandergaard, Eds., Technomic Publishing Co, Lancaster, 1995.

[47] J. Muralikrishna and K. R. Rajagopal, A Thermodynamic Framework for the constitutive modeling Asphalt Concrete, Part1: Theoretical considerations. *ASCE Journal of Materials*, accepted.

[48] P. M. Naghdi, A critical review of the state of finite plasticity. *ZAMP*, **41** (1990), 315-393.

[49] K. Nogami, S. Murakami, K. Katayama, and K. Kobayashi, An optical study on shear-induced crystallization in polymers. *Bulletin of the Institute of Chemistry Research, Kyoto University*, **55** (1977), 277-236.

[50] A. Peterlin, Crystallization from a strained melt. *Polymer Engineering and Science*, **16** (1976), 126-137.

[51] K. R. Rajagopal and A. S. Wineman, A constitutive equation for nonlinear solids which undergo deformation induced microstructural changes. *International Journal of Plasticity*, **8** (1992), 385-395.
[52] K. R. Rajagopal, Multiple configurations in continuum mechanics., in *Reports of the Institute for Computational and Applied Mechanics*. University of Pittsburgh 1995.
[53] K. R. Rajagopal and A. R. Srinivasa, On the inelastic behavior of solids: Part-I- Twinning. *International Journal of Plasticity*, **11** (1995), 653-678.
[54] K. R. Rajagopal and L. Tao, *Mechanics of Mixtures*. World Scientific, River Edge, NJ 1995.
[55] K. R. Rajagopal and A. R. Srinivasa, Inelastic behavior of materials: Part-I- Theoretical underpinnings. *International Journal of Plasticity*, **14** (1998), 945- 967.
[56] K. R. Rajagopal and A. R. Srinivasa, On the thermodynamics of shape memory wires. *ZAMP*, **50** (1999), 459-496.
[57] K. R. Rajagopal and A. R. Srinivasa, A thermodynamic frame-work for rate type fluid models. *Journal of Non-Newtonian Fluid Mechanics*, **88** (2000), 207-227.
[58] K. R. Rajagopal and A. R. Srinivasa, Modeling anisotropic fluids within the framework of bodies with multiple natural configurations. *Journal of Non- Newtonian Fluid Mechanics*, in press (2001).
[59] I. J. Rao and K. R. Rajagopal, Phenomenological modeling of crystallization in polymers using the notion of multiple natural configurations. *Interfaces and Free Boundaries*, **2** (2000), 73-94.
[60] I. J. Rao and K. R. Rajagopal, A Study of Strain Induced Crystallization in Polymers. *International Journal of Solids and Structures*, **38** (2001), 1149-1167.
[61] L. I. Rubinstein, *The Stefan Problem*. Translations of mathematics monographs. Vol. 27. A.M.S., Providence, RI 1971.
[62] J. M. Schultz, Theory of crystallization in high-speed spinning. *Polymer Engineering and Science*, **31** (1991), 661-666.
[63] C. H. Sherwood, F. P. Price, and R. S. Stein, The effects of shear on the crystallization kinetics of poly(ethylene oxide) and poly(e-caprolactone) melts. *Journal of Polymer Science, Polymer Symposium*, **63** (1978), 77-94.
[64] K. J. Smith, Crystalline growth due to stress induced nucleation. *Polymer Engineering and Science*, **16** (1976), 169-175.
[65] K. J. Smith, Inclusion of mobile crosslinks and lateral crystalline growth in the theory of stress induced crystallization. *Journal of Polymer Science, Part B, Polymer Physics*, **21** (1983), 45-53.
[66] A. J. M. Spencer, *Deformations of Fibre-Reinforced Materials.* Clarendon Press, Oxford 1972.
[67] J. Stefan, On the theory of formation of ice, in particular in the polar sea. *Annalen der Physik und Chemie*, (Wiedemann), **42** (1891), 269-286.
[68] P. Supaphol and J. E. Spruiell, Nonisothermal bulk crystallization studies of high density polyethylene using light depolarizing microscopy. *Journal of Polymer Science: Part B: Polymer Physics*, **36** (1998), 681-692.
[69] C. Truesdell, Sulle basi della thermomeccanica. *Rendiconti Lincei*, **22** (1957), 33-38.
[70] C. Truesdell and W. Noll, *The Non-Linear Field Theories of Mechanics*, 2nd edition. Springer-Verlag, Berlin 1992.
[71] R. E. Ulrich and F. P. Price, Morphology development during shearing of poly(ethylene oxide) melts. *Journal of Applied Polymer Science*, **20** (1976), 1077-1093.
[72] A. K. van der Vegt and P. P. A. Smit, Crystallization phenomena in flowing polymers. *Society of Chemical Industry*, **26** (1967), 313-325.
[73] J. L. White, Structure development in polymer processing. *Pure & Applied Chemistry*, **55** (1983), 765-776.
[74] J. L. White and J. E. Spruiell, The specification of orientation and its development in

polymer processing. *Polymer Engineering and Science*, **23** (1983), 247-256.
[75] A. S. Wineman and K. R. Rajagopal, On a constitutive theory for materials undergoing microstructural changes. *Archives of Mechanics*, **42** (1990), 53-75.
[76] M. D. Wolcowicz, Nucleation and crystal growth in sheared poly(1-butene) melts. *Journal of Polymer Science, Polymer Symposium*, **63** (1978), 365-382.
[77] B. Wunderlich, *Macromolecular Physics. Vol. 2. Crystal Nucleation, Growth and Annealing*. Academic Press, New York 1976.
[78] A. Ziabicki, Theoretical analysis of oriented and non isothermal crystallization. I. Phenomenological considerations. Isothermal crystallization accompanied by simultaneous orientation or disorientation. *Colloid and Polymer Science*, **252** (1974), 207-221.
[79] A. Ziabicki, *Fundamentals of Fiber Formation*. John Wiley and Sons, New York 1976.
[80] A. Ziabicki, Crystallization of polymers in variable external conditions. *Colloid and Polymer Science*, **274** (1996), 209-217.

I. J. Rao
Department of Mechanical Engineering
New Jersey Institute of Technology
University Heights
Newark, NJ 07102
USA

K. R. Rajagopal
Department of Mechanical Engineering
Texas A&M University
College Station
TX 77804
USA

(Received: July 2, 2001)